Marine Biology (2019) 166:80
https://doi.org/10.1007/s00227-019-3528-y

ORIGINAL PAPER

Combined effects of simulated acidification and hypoxia on the harmful dinoflagellate *Amphidinium carterae*

Alexandra R. Bausch[1,2,3] · Andrew R. Juhl[2,3] · Natalie A. Donaher[4] · Amanda M. Cockshutt[4]

Received: 9 November 2018 / Accepted: 11 May 2019 / Published online: 18 May 2019

Abstract

Hypoxia and acidification frequently co-occur in coastal marine ecosystems, and will likely become more intense and persistent with anthropogenic climate change. Although the separate effects of these stressors have previously been described, their combined effects on marine phytoplankton are currently unknown. In this novel study, multi-stressor incubation experiments using the harmful dinoflagellate, *Amphidinium carterae*, examined the effects of acidification and hypoxia both individually and in combination. Long-term (7 days) and short-term (6 h) experiments under controlled carbon dioxide (CO_2) and oxygen (O_2) conditions examined the interactive effects of the stressors and the physiological mechanisms driving their interaction. In the long-term experiment, synergistically negative effects were observed for *A. carterae* growth, photosynthesis, carbon fixation, nitrate uptake, and photosynthetic efficiency (F_v/F_m) under combined high CO_2 (low pH) and low O_2 conditions. In the short-term experiment, delayed recovery of photosystem II (PSII) reaction centers was observed following photoinhibition, suggesting that high CO_2 and low O_2 conditions negatively affect photosynthesis in *A. carterae* even after relatively short exposures. Although high CO_2, low O_2 conditions should decrease photorespiration and favor carbon fixation by the key photosynthetic enzyme ribulose-1,5-bisphosphate-carboxylase/oxygenase (RuBisCO), these findings demonstrate that the affinity of RuBisCO for CO_2 relative to O_2 alone does not predict phytoplankton responses to CO_2 and O_2 conditions in vivo, complicating predictions of phytoplankton community responses to hypoxia and acidification. Results of these experiments suggest that the combination of low pH and O_2 concentrations may negatively impact the growth of some harmful dinoflagellates in coastal marine ecosystems.

Introduction

'Ocean acidification' frequently refers to the ongoing decrease in ocean pH and change in seawater carbonate chemistry driven by oceanic uptake of anthropogenic carbon dioxide (CO_2) from the atmosphere (Caldeira and Wickett 2003; Doney et al. 2009). By the end of this century, atmospheric CO_2 concentrations are predicted to increase up to 1150 ppmv (IPCC 2013), causing a decrease in the average surface ocean pH by 0.3–0.5 units (Caldeira and Wickett 2005). These high CO_2 (low pH) conditions will have significant, wide-ranging consequences for many marine organisms (Guinotte and Fabry 2008; Doney et al. 2009; Kroeker et al. 2013).

Coastal hypoxia is another critical threat to marine ecosystem health occurring in concert with ocean acidification. Low oxygen (O_2) conditions commonly occur in aquatic ecosystems as a result of microbial metabolic processes (Keeling et al. 2010; Gobler and Baumann 2016). Hypoxic conditions, operationally defined as O_2 concentrations < 62.5 µmol

Responsible Editor: S. Shumway.

Reviewed by P. Cardol.

Electronic supplementary material The online version of this article (https://doi.org/10.1007/s00227-019-3528-y) contains supplementary material, which is available to authorized users.

✉ Alexandra R. Bausch
abausch@stanford.edu

[1] Department of Earth System Science, Stanford University, Stanford, CA 94305, USA

[2] Lamont–Doherty Earth Observatory, Columbia University, Palisades, NY 10964, USA

[3] Department of Earth and Environmental Sciences, Columbia University, Palisades, NY 10964, USA

[4] Mount Allison University, Sackville, NB E4L 1E4, Canada

L^{-1} (Vaquer-Sunyer and Duarte 2008; Cai et al. 2011), are often exacerbated by eutrophication in coastal waters. High nutrient inputs during eutrophication typically lead to algal blooms, followed by high microbial respiration and hypoxia as the organic matter fixed during the bloom is decomposed. Over the course of this century, the so-called hypoxic 'dead zones' are predicted to significantly expand as a result of eutrophication in highly populated coastal zones (Diaz and Rosenberg 2008; Rabalais et al. 2010; Gruber 2011). Hypoxia has serious negative impacts on marine organisms and ecosystems, since its effects can be lethal for many species (Diaz and Rosenberg 2008).

Due to the metabolic connection between O_2 consumption and CO_2 release, acidification and hypoxia are functionally related to each other (e.g., Cai et al. 2011; Melzner et al. 2013; Wallace et al. 2014). Acidification driven by microbial respiration is sometimes referred to as 'coastal acidification' to differentiate the process from acidification driven by anthropogenic CO_2 emissions (Wallace et al. 2014). While ocean acidification is driven by the uptake of atmospheric CO_2, coastal acidification is controlled by the biological production of CO_2. The same metabolic processes that drive hypoxia also release CO_2, thereby decreasing seawater pH (Cai et al. 2011; Sunda and Cai 2012; Wallace et al. 2014). For example, in stratified, eutrophic waters, high O_2 and low CO_2 conditions can occur near the surface due to photosynthesis, together with low O_2 and high CO_2 conditions at depth due to stratification and high microbial respiration (Diaz and Rosenberg 2008; Cai et al. 2011). With sufficient nutrient loading, however, hypoxic and acidic conditions can characterize the entire water column (e.g., Wallace et al. 2014; Gobler and Baumann 2016). In addition, low O_2, high CO_2 conditions occur naturally in deeper waters in oxygen minimum zones (OMZs; Rabalais et al. 2010; Gobler and Baumann 2016). Both natural upwelling along coastal regions (e.g., the Oregon coast) and anthropogenic climate change can expand hypoxic and acidic waters within OMZs into surface waters (Diaz and Rosenberg 2008; Rabalais et al. 2010; Gobler and Baumann 2016). It is predicted that the frequency and intensity of low O_2, low pH zones will increase over the course of this century with enhanced climatic warming and eutrophication (Keeling et al. 2010; Rabalais et al. 2010). In addition, due to the strong coupling of hypoxia and coastal acidification in combination with ocean acidification, coastal waters with low O_2 may become disproportionately more acidic (Cai et al. 2011; Melzner et al. 2013).

Despite the co-occurrence of acidification and hypoxia in many coastal marine ecosystems and the likelihood of significant changes by the end of this century, little is known about the interactive effects of decreasing pH in conjunction with decreasing O_2 on marine organisms (Baumann 2016). While many studies have examined the individual effects of low seawater pH (e.g., Guinotte and Fabry 2008; Doney et al. 2009; Kroeker et al. 2013) or low dissolved O_2 (e.g., Diaz and Rosenberg 2008; Vaquer-Sunyer and Duarte 2008; Rabalais et al. 2010), few studies have examined the combined effects of these environmental stressors (e.g., Pope 1975; Kitaya et al. 2008; Bagby and Chisholm 2015). Some of the studies investigating the effects of hypoxia inadvertently manipulated CO_2 and O_2 conditions together by bubbling with nitrogen gas (as discussed by Gobler et al. 2014). However, it is essential to use controlled incubations to examine the effects of CO_2 and O_2 together, since the combination of acidification and hypoxia may have stronger negative effects on some marine organisms than the sum of each individual stressor (Guinotte and Fabry 2008; Baumann 2016; Gobler and Baumann 2016). In fact, the small number of experimental studies that have examined combined CO_2 and O_2 show some strong interactive effects or unexpected synergies in both marine animals (e.g., fish and invertebrates; Gobler et al. 2014; DePasquale et al. 2015; Baumann 2016) and algae (e.g., symbiotic dinoflagellates and cyanobacteria; Kitaya et al. 2008; Bagby and Chisholm 2015). Among algae, it is possible that such synergistic effects may develop as a result of the key photosynthetic enzyme ribulose-1,5-bisphosphate-carboxylase/oxygenase (RuBisCO), since RuBisCO is affected by both ambient CO_2 and O_2 concentrations (e.g., Peterhansel et al. 2010).

When the CO_2:O_2 ratio at the active site is high, RuBisCO uses CO_2 as a substrate for carbon fixation (Peterhansel et al. 2010). However, when the CO_2:O_2 ratio decreases, RuBisCO uses O_2 as a substrate instead of CO_2 and photorespiratory activity increases (Bowes et al. 1971; Foyer and Noctor 2000). Thus, maximal rates of photorespiration should occur under low CO_2, high O_2 conditions (Foyer and Noctor 2000). Since photorespiration is an energetically expensive diversion from carbon fixation, it is often perceived as a 'wasteful' process (Peterhansel et al. 2010). However, photorespiration serves an important role in cell physiology by balancing the light-dependent and -independent reactions of photosynthesis (Takeba and Kozaki 1998; Bagby and Chisholm 2015). Photorespiration also removes metabolic intermediates that inhibit the Calvin–Benson–Bassham (CBB) cycle (e.g., 2-phosphoglycolate), protects cells from photoinhibition during stress conditions, and supports cell defense mechanisms (Bauwe et al. 2010, 2012; Peterhansel et al. 2010).

The capacity of RuBisCO to differentiate between the substrates CO_2 and O_2 (i.e., RuBisCO specificity; Tortell 2000) is determined by its distinct structural form (Tabita et al. 2007) and the availability of CO_2 relative to O_2 (Foyer and Noctor 2000). RuBisCO CO_2:O_2 specificity is highly taxon-specific and correlated with the atmospheric conditions of CO_2 and O_2 during the evolution of various phytoplankton lineages (Tortell 2000). Most dinoflagellates

contain Form II RuBisCO (Jenks and Gibbs 2000), which is particularly inefficient at discriminating between CO_2 and O_2 (Tabita et al. 2007). This structural form of RuBisCO may cause dinoflagellates to be particularly sensitive to ambient CO_2 and O_2 conditions compared to some other phytoplankton taxa (Tortell 2000; Eberlein et al. 2014). However, photosynthetic organisms with low RuBisCO specificity can employ carbon concentrating mechanisms (CCMs) to accumulate higher CO_2 concentrations near their RuBisCO molecules (Raven et al. 2008), potentially avoiding the need for high specificity except under unusually low CO_2 concentrations.

Among the dinoflagellates that are likely sensitive to the combination of CO_2 and O_2 in coastal waters, harmful algal bloom (HAB) species are of particular interest. Given their low RuBisCO specificity, their potential for deleterious impacts, and their connection to high CO_2 and low O_2 conditions in eutrophic, coastal systems (Fu et al. 2012), it is essential to understand the interactive impacts of acidification and hypoxia on toxin-producing HAB dinoflagellates, in addition to other marine photoautotrophs.

Amphidinium carterae is a cosmopolitan, bloom-forming dinoflagellate found in temperate-to-tropical coastal and estuarine waters (Steidinger and Jangen 1996; Hargraves and Maranda 2002). It is considered a HAB species (Murray et al. 2012) and is known to produce toxic ichthyotoxins (Huang et al. 2009) and hemolytic substances (Echigoya et al. 2005). Since *A. carterae* has ecological importance, particularly in coastal marine environments (Hargraves and Maranda 2002; Murray et al. 2012), and has published RuBisCO specificity measurements (Whitney and Andrews 1998), it is an ideal model organism to examine the physiological effects of acidification and hypoxia. The measured RuBisCO substrate specificity of *A. carterae* is higher than that of any other Form II RuBisCO found in anaerobic bacteria (Whitney and Andrews 1998). However, it is extremely low compared to that of other eukaryotic photoautotrophs, indicating a diminished affinity for CO_2 relative to O_2 (Whitney and Andrews 1998; Young et al. 2016). It is, therefore, likely that *A. carterae* uses a CCM to concentrate CO_2 at the active site of RuBisCO (Burns and Beardall 1987; Badger et al. 1998; Whitney and Andrews 1998; Jenks and Gibbs 2000), particularly given that dinoflagellates carry many genes putatively involved in CCMs (Hennon et al. 2017). Since *A. carterae* lacks external carbonic anhydrase (CA), its capacity for active bicarbonate uptake may be limited, however (Dason et al. 2004), and its growth may be stimulated at high CO_2 concentrations (Fu et al. 2012).

The primary objective of this study was to examine the interactive effects of acidification and hypoxia on *A. carterae*. Factorial experiments using *A. carterae* examined the impacts of simulated hypoxia and acidification both individually and in combination. Cultures were maintained in up to four experimental treatments: (1) control, which reflects current atmospheric levels of CO_2 and O_2; (2) high CO_2 (low pH), which reflects ocean acidification conditions associated with 'worst-case scenario' CO_2 levels by 2100 (IPCC 2013); (3) low O_2, which reflects coastal hypoxic conditions predicted to intensify by 2100 (Rabalais et al. 2010); and (4) combined high CO_2 and low O_2, which reflects co-occurring coastal acidification and hypoxia (Wallace et al. 2014). Both long-term (7 days) and short-term (6 h) incubations were performed under these controlled CO_2 and O_2 conditions. Since cellular carbon metabolism is controlled by the concentrations of CO_2 and O_2 at the active site of RuBisCO, as well as the CO_2:O_2 specificity of RuBisCO (Foyer and Noctor 2000; Tortell 2000), in vitro RuBisCO specificity was hypothesized to predict *A. carterae* organismal responses to CO_2 and O_2 concentrations. Specifically, elevated CO_2 and low O_2 conditions were predicted to particularly benefit *A. carterae* growth, metabolism, and physiology, since these conditions should drive carbon fixation and prevent photorespiration. Since in vitro RuBisCO specificity of *A. carterae* could not be used to predict responses to CO_2 and O_2 conditions in vivo, the second research objective was to investigate the physiological mechanism driving synergistic, negative effects at high CO_2 and low O_2 on an organismal level. This study was the first to examine the synergistic effects of acidification and hypoxia on a species of harmful algae.

Materials and methods

Algal culture and medium

Axenic cultures of *Amphidinium carterae* (CCMP 1314; Hulburt 1957), obtained from the National Center for Marine Algae and Microbiota, were grown in L1 medium without added silicate (Guillard and Hargraves 1993). Medium was prepared using 0.2-µm-filtered (Pall Acropak), autoclave-sterilized coastal seawater collected from the University of Connecticut Avery Point Campus, Connecticut, USA (salinity = 32). Cultures were maintained at a temperature of 20 °C and a light intensity of 100 µmol quanta m^{-2} s^{-1} (Dixon and Syrett 1988) with a photoperiod of 13 h light:11 h dark.

During all experiments, *A. carterae* cultures were incubated under up to four experimental treatments: (1) control (400 ppmv CO_2 and 21% O_2); (2) high CO_2 (1200 ppmv CO_2 and 21% O_2); (3) low O_2 (400 ppmv CO_2 and 2% O_2); and (4) combined high CO_2 and low O_2 (1200 ppmv CO_2 and 2% O_2). All experimental designs were consistent with recommendations for ocean acidification experiments in Cornwall and Hurd (2016). Experimental treatment conditions in the medium were monitored over time (Table 1, Tables S1, S2).

Table 1 Average treatment conditions in the long-term (7 days) and short-term (6 h) *Amphidinium carterae* experiments (mean ± SEM), including number of individual bottles per treatment (*N*), irradiance (*I*), temperature (*T*), salinity (*S*), pH on the total scale (pH_T), total alkalinity (A_T), partial pressure of carbon dioxide (pCO_2), and dissolved oxygen concentration (O_2)

Treatment	*N*	*I* (μmol m^{-2} s^{-1})	*T* (°C)	*S*	pH_T	A_T (μmol kg^{-1})	pCO_2 (μatm)	O_2 (μmol L^{-1})
Long-term experiment (following acclimation)								
Control	4	104.4 ± 6.4	20.0 ± < 0.1	32	8.04 ± 0.02	2030.9 ± 6.9	331.4 ± 10.9	239.7 ± 10.1
High CO_2	4	102.6 ± 9.4	19.9 ± < 0.1	32	7.64 ± 0.01	2055.5 ± 9.3	1129.0 ± 36.3	251.8 ± 5.7
Low O_2	4	103.0 ± 11.0	20.0 ± < 0.1	32	7.91 ± 0.01	1998.4 ± 6.2	512.3 ± 16.9	62.9 ± 5.8
High CO_2, low O_2	4	102.9 ± 7.9	20.0 ± 0.0	32	7.60 ± 0.02	2019.4 ± 5.1	1080.5 ± 44.1	59.7 ± 5.0
Short-term experiment examining metabolism								
Control	4	106.5 ± 6.8	19.9	32	7.93 ± < 0.01	1993.1 ± 3.2	489.9 ± 6.6	254.6 ± 4.0
High CO_2	4	104.3 ± 8.3	20.0	32	7.63 ± < 0.01	1993.1 ± 3.2	1056.7 ± 7.4	253.0 ± 2.5
Low O_2	4	102.5 ± 7.1	20.0	32	7.90 ± < 0.01	1993.1 ± 3.2	519.9 ± 3.0	65.9 ± 0.7
High CO_2, low O_2	4	101.3 ± 6.3	20.1	32	7.60 ± < 0.01	1993.1 ± 3.2	1111.1 ± 12.6	66.2 ± 0.8
Short-term experiment examining photophysiology								
Control	3	98.7 ± 1.8	20.0	32	7.92 ± 0.01	1993.1 ± 3.2	496.7 ± 13.3	247.0 ± 2.5
High CO_2, low O_2	3	95.0 ± 2.0	20.0	32	7.51 ± < 0.01	1993.1 ± 3.2	1392.5 ± 11.3	52.8 ± 1.0

Long-term effects on growth, metabolism, and physiology

Before both the long-term acclimation and grow-out, the medium in each culture flask (2 L polycarbonate) was bubbled for at least 1 h using high-efficiency particulate air- (HEPA-) filtered three-component compressed gas mixtures of CO_2 (400 or 1200 ppmv), O_2 (2 or 21%), and N_2 (balance). When the desired pH and O_2 levels were reached, bubbling was stopped and *A. carterae* cells were inoculated in the gas-amended media. To maintain constant pH and O_2 conditions while preventing shear stress from bubbling (e.g., Juhl and Latz 2002), the culture flask headspaces were continuously purged with the corresponding compressed gas mixture. Gas flow rates were maintained at 0.1 LPM using needle valve flow meters (Cole Parmer). Flasks were fitted with porous stoppers to allow gas to escape and swirled continuously on orbital shaker tables (45 RPM). Comparison to unshaken flasks suggested that this level of shaking did not affect *A. carterae* growth rates, but did enhance gas diffusion.

The long-term experiment lasted 7 days. *A. carterae* cells were initially acclimated for 3 days under controlled pH and O_2 conditions with initial cell concentrations ranging from 4.4 to 6.6×10^3 cells mL^{-1} in different treatments (400 mL medium in each flask). Acclimated cultures were then used to inoculate four replicate flasks per treatment (i.e., 16 flasks in total; 1.2 L medium in each flask) with initial cell concentrations ranging from 0.9 to 1.2×10^3 cells mL^{-1}. Cultures were maintained for another 4 days under the same conditions as the acclimation period with final cell concentrations ranging from 0.6 to 1.5×10^4 cells mL^{-1}. Low cell concentrations minimized changes in pH and O_2 over time due to algal metabolism, and were intended to be comparable to typical in situ concentrations during blooms.

Subsamples of *A. carterae* were collected daily from each flask, preserved in acid Lugol's solution (2% final concentration), and counted at 100 × magnification (Axiostar Plus microscope, Zeiss). Growth rates in each flask were determined by fitting the exponential growth equation to cell counts during the last four time points ($R^2 > 0.950$ in each case).

Estimates of in vivo chlorophyll *a* were determined daily from each flask using a handheld active fluorometer (*Aqua*Flash, Turner Designs), using filtered culture medium for blank correction. Extracted chlorophyll *a* concentrations were measured from each flask at the end of the 7-day incubation. Culture samples (25 mL) were filtered onto GF/F filters (Whatman), stored at − 20 °C, and extracted in 10 mL of 90% acetone. Chlorophyll *a* concentrations of the extract were measured using a handheld fluorometer (*Aqua*Fluor, Turner Designs) before and after acidification (Strickland and Parsons 1972). The measured in vivo and extracted chlorophyll *a* values at the end of the 7-day incubation were linearly correlated ($R^2 = 0.83$, $n = 16$).

Measurements of dark minimum chlorophyll *a* fluorescence (F_o) and dark maximum fluorescence (F_m) were determined daily from each flask using the *Aqua*Flash fluorometer, using filtered culture medium for blank correction. Maximum quantum yield (F_v/F_m) was then calculated by the following:

$$F_v/F_m = \frac{F_m - F_o}{F_m}. \quad (1)$$

Dissolved O_2 concentrations were determined by subsampling from each flask into glass scintillation vials fitted with non-invasive O_2 sensor spots (PSt3, PreSens). Using

these vials, O_2 concentrations were measured daily using a single-channel fiber optic O_2 transmitter with temperature, pressure, and salinity compensation (Fibox 4, PreSens).

Dark respiration and net photosynthesis were determined from each flask at the end of the 7-day incubation by measuring changes in O_2 over 5 h in dark and light (100 µmol quanta m^{-2} s^{-1}) scintillation vials, respectively. Gross photosynthesis was estimated by summing net photosynthesis and dark respiration. Specifically, linear regressions of O_2 concentrations through time were used to calculate rates of dark respiration per cell (linear regressions from all treatments, $R^2 > 0.6566$), gross photosynthesis per cell ($R^2 > 0.9471$), and net photosynthesis per cell ($R^2 > 0.9479$; e.g., Fig. S2). Note that this calculation assumes equivalent light and dark respiration rates, and does not account for photorespiration. Slow diffusion into the scintillation vials in the low O_2 treatments could not be avoided, and thus, low O_2 measurements were corrected by the rate of diffusion (1.83 µmol O_2 L^{-1} h^{-1}; $R^2 = 0.9652$, $n = 3$), measured in sterile seawater.

Measurements of pH on the total hydrogen scale (pH_T) were obtained daily from each flask using a modified version of the spectrophotometric method with 1 mL of sample and two 5-µL aliquots of *m*-cresol purple indicator (adapted from SOP 6b; Dickson et al. 2007). Spectroscopic measurements were performed using a double-beam UV–Vis spectrophotometer (UV-1800, Shimadzu), fitted with 20-mm path-length special optical glass spectrophotometric cells (18B-SOG-20, Starna). To ensure analytical quality control, sample pH values were calibrated against that of Tris buffer reference standard (Andrew Dickson, Scripps Institution of Oceanography; batch T28).

Total alkalinity (A_T) measurements were obtained from bulk medium at the beginning and from each flask at the end of the 7-day incubation using the potentiometric titration method (SOP 3b; Dickson et al. 2007). Samples (140 mL) were fixed with 20 µL saturated mercuric chloride solution ($0.01\%_{w/v}$ $HgCl_2$ final concentration) and analyzed using an automatic potentiometric titrator (888 Titrando, Metrohm) with Tiamo software (version 2.5). Sample A_T values were calibrated against that of certified CO_2 reference material (Andrew Dickson, Scripps Institution of Oceanography; batches 149 and 156).

The partial pressure of CO_2 (pCO_2) in each flask was calculated from temperature, salinity, pH_T, and A_T data using CO_2calc (Robbins et al. 2010) with the dissociation constants of Mehrbach et al. (1973), as refit by Dickson and Millero (1987).

Nutrient samples were collected from bulk medium at the beginning and from each flask at the end of the 7-day incubation. Samples were 0.22-µm syringe-filtered and stored at − 20 °C. Concentrations of ammonium, nitrate, nitrite, and phosphate were measured at the Nutrient Analytical Services Laboratory at the Chesapeake Biological Laboratory using a discrete analyzer (Konelab Aquakem 250, Thermo Scientific). Briefly, dissolved inorganic ammonium, nitrite, and orthophosphate were determined using automated colorimetry; dissolved inorganic nitrate plus nitrite was determined using the enzyme catalyzed reduction method.

Stable isotopes (^{13}C and ^{15}N) were used as tracers in a labeling incubation experiment to quantify ^{13}C and ^{15}N labeling in harvested cells due to carbon and nitrogen uptake. At the end of the 7-day incubation, subsamples (200 mL) from each flask were incubated under treatment conditions with a final concentration of 1 mM ^{13}C-labeled sodium bicarbonate (< 50% of DIC) and 0.5 mM ^{15}N-labeled sodium nitrate (< 50% of L1 nitrate) for 3 h. At the end of the 3-h incubation, samples (150 mL) were filtered onto combusted GF/F filters (Whatman), stored at − 20 °C, and freeze-dried.

Isotopic analyses were performed at the Stable Isotope Laboratory at Lamont–Doherty Earth Observatory. Sample filters were weighed, encapsulated into tin capsules, and stored in a desiccator until analysis. Briefly, $\delta^{13}C$ and $\delta^{15}N$ signatures were analyzed via the combustion method using an elemental analyzer (ECS 4010, Costech) fitted with a universal continuous flow interface (ConFlo IV, Thermo Scientific) and an isotope ratio mass spectrometer (Delta V, Thermo Scientific). Carbon and nitrogen contents were calibrated by acetanilide. Carbon isotope ($\delta^{13}C$) measurements were calibrated by three-point regression of natural isotope standards (USGS40, USGS41, and USGS24). Similarly, nitrogen isotope ($\delta^{15}N$) measurements were calibrated by standard regression (USGS40, USGS41, and IAEA-N3). It is important to note that these three-point regressions using natural abundance isotope standards were extrapolated to determine enriched signatures following ^{13}C and ^{15}N labeling. Therefore, the enriched $\delta^{13}C$ and $\delta^{15}N$ data may be skewed and may have larger errors than those reported here. It is important to note that the $\delta^{13}C$ and $\delta^{15}N$ signatures were compared only among treatments in this study and, therefore, represent relative measures of carbon fixation and nitrate uptake, respectively.

Samples for total protein and RuBisCO content were collected from each flask at the end of the 7-day incubation. *A. carterae* culture samples (100 mL) were filtered onto 0.8-µm polycarbonate filters (Nucleopore, Whatman), folded cell-to-cell, cryo-preserved in liquid nitrogen, and stored at − 80 °C.

Protein extractions were performed using the FastPrep-24 and bead lysing 'matrix D' (MP Biomedicals), with three cycles of 60 s at 6.5 m s^{-1} in 500 µL of 1 × extraction buffer (AS08 300, Agrisera) containing 0.4 mM 4-(2-aminoethyl) benzenesulfonyl fluoride hydrochloride (AEBSF; Bioshop Canada), and then spun at 16,000*g* for 8 min. The supernatant was assayed for total protein content using the detergent compatible (DC) assay kit against bovine γ-globulin (BGG) standard (Bio-Rad), and then prepared for electrophoresis based on equivalent total protein loads (2 µg)

using 1 × lithium dodecyl sulfate (LDS) sample buffer (Life Technologies) and 50 mM dithiothreitol (DTT) heated for 5 min at 70 °C. Separation of proteins was performed in a Bolt 4–12% Bis Tris sodium dodecyl sulfate polyacrylamide gel electrophoresis (SDS-PAGE) gel (Life Technologies) with 200 V power for 40 min alongside a molecular marker (MagicMark, Life Technologies), and then transferred to a polyvinylidene difluoride (PVDF) membrane (Bio-Rad) for 60 min using 30 V. Each gel also had a four-point quantitation curve using the large subunit of RuBisCO (RbcL) Form II (AS15 2955S, Agrisera).

Membranes were blocked for 1 h in $2\%_{w/v}$ enhanced chemiluminescence (ECL) blocking agent (GE Healthcare) dissolved in Tris-buffered saline and Tween (TBS-T, containing 20 mM Tris, 137 mM NaCl, $0.1\%_{v/v}$ Tween-20), then incubated in 1:20,000 rabbit polyclonal anti-RbcL Form II antibody for 1 h (AS15 2955, Agrisera), and finally in 1:20,000 goat anti-rabbit IgG horseradish peroxidase (HRP) conjugated antibody (AS09 602, Agrisera) for 1 h. After each antibody incubation, membranes were rinsed with TBS-T solution five times. Chemiluminescent images were obtained using ECL Select reagent (GE Healthcare) and a VersaDoc charge coupled device (CCD) imager (Bio-Rad). Band densities for samples were determined against the standard curve using ImageLab software (version 4.0, Bio-Rad).

Short-term impacts on metabolism

The short-term experiment was performed over 6 h under identical treatment conditions and using the same basic experimental design as the long-term experiment but without an acclimation period. Stock *A. carterae* culture was transferred to four replicate flasks per treatment using the same bottles as the long-term experiment (i.e., 16 flasks in total; 100 mL medium in each flask). Initial cell counts (ranging from 6.6 to 8.4×10^3 cells mL^{-1}), in vivo chlorophyll *a*, F_v/F_m, O_2, pH_T, A_T, and pCO_2 were measured as described above. After the 6-h incubation, dark respiration, gross photosynthesis, net photosynthesis, and F_v/F_m were determined again as described above.

Short-term impacts on photophysiology

An additional short-term experiment examined *A. carterae* photophysiology under the two treatment conditions that yielded the most extreme differences in *A. carterae* growth and metabolism: (1) control and (2) combined high CO_2, low O_2. Stock *A. carterae* cells were inoculated into three replicate flasks per treatment (i.e., 6 flasks in total; 54 mL medium in each 25-cm^2 Nunc polystyrene screw-cap cell culture flask). The initial cell counts (ranging from 3.3 to 4.8×10^4 cells mL^{-1}), in vivo chlorophyll *a*, F_v/F_m, O_2, and pH_T were determined as described above. Measured A_T from the previous short-term experiment was used to calculate pCO_2 values, since the same medium was used. After 6 h of incubation while purging the headspace, F_v/F_m was measured as described above. In addition, chlorophyll fluorescence-based light response and recovery curves (e.g., Brooks and Niyogi 2011) were measured from each flask using a xenon pulse amplitude modulated (PAM) fluorometer (Xe-PAM, Walz), using filtered culture medium for blank correction. Cultures were subsampled into fluorescence cuvettes, sealed, and dark-adapted for 5 min (Possmayer et al. 2011). Samples were exposed to a very low-intensity measuring light (Schreiber et al. 1993) pulsed at 2 Hz to measure Fo, followed by a saturating light flash (4000 µmol quanta m^{-2} s^{-1}) for 0.8 s to measure Fm (Cao et al. 2011; Possmayer et al. 2011). Samples were then illuminated with an actinic halogen lamp for 1 min at a light intensity similar to ambient conditions (~90 µmol quanta m^{-2} s^{-1}) to achieve steady state. The light response was then measured by illuminating each sample at seven additional, increasing light levels up to ~1700 µmol quanta m^{-2} s^{-1} for 1 min each. Saturation flashes were superimposed every 1 min (Possmayer et al. 2011) to measure steady-state (*F*) and maximum fluorescence under actinic light (F_m'). Effective quantum yield under actinic illumination (F_v'/F_m') was calculated by the following:

$$F_v'/F_m' = \frac{F_m' - F}{F_m'}. \quad (2)$$

The relative electron transport rate (ETR) was also calculated at each actinic light level (as in Wu et al. 2010) by the following:

$$\mathrm{ETR} = Fv'/Fm' \times I \times 0.84 \times 0.5, \quad (3)$$

where *I* is the actinic light intensity, the coefficient 0.84 indicates that 84% of incident light was absorbed by the sample, and the coefficient 0.5 indicates that 50% of absorbed quanta reached photosystem II (PSII). Note that ETR was not normalized to biomass and, therefore, represents only a relative measure of photosynthesis. Plotting relative ETR against actinic light intensity provided photosynthesis-irradiance (PI) curves for each sample. Immediately following the light response measurements, dark recovery of photophysiology was assessed by six additional measurements of F_v'/F_m' spaced over the next 19 min, while samples otherwise remained in the dark. Non-photochemical quenching (NPQ) was determined during dark recovery:

$$\mathrm{NPQ} = \frac{F_m - F_m'}{F_m'}. \quad (4)$$

All PAM data (used in Eqs. 2–4) were obtained using WinControl software (version 2.08; Walz).

Statistical analyses

Data were analyzed and plotted using Prism GraphPad software (version 7). Linear regressions, as well as one- and two-way analyses of variance (ANOVA) with Fisher's least significant difference (LSD) post hoc tests were used to determine significant differences in measurements among treatments. Note that many of the figures use letters to denote statistical significance: different letters indicate statistical significance compared to other treatments in the same figure panel.

Results

Long-term effects on growth, metabolism, and physiology

Combined CO_2 and O_2 conditions had significant effects on *Amphidinium carterae* growth rates (based on cell counts; Fig. S1) over the 7-day exposure [one-way ANOVA, $F(3,12) = 50.23$, $p < 0.0001$; Fig. 1]. The combination of high CO_2 and low O_2 conditions had synergistically negative effects on *A. carterae* growth (Fisher's LSD multiple comparison, $p < 0.0001$; Table 2). This effect was not the result of CO_2 or O_2 conditions separately, since high CO_2 stimulated *A. carterae* growth ($p = 0.0027$), while low O_2 had no significant impact on growth. Note that all responses of *A. carterae* to treatment conditions were defined as synergistic when the combined effects of multiple drivers were greater than the additive effects of individual drivers (Table 2; Breitburg et al. 2015).

Daily measurements of O_2 and pH_T after the acclimation period remained relatively constant over time in each treatment (Table 1, Table S1). Macronutrient concentrations did not limit exponential growth of *A. carterae* (Table S2). At the final time point, nitrate and phosphate concentrations in all flasks were above 1.5×10^{-4} M and 3.2×10^{-5} M, respectively (data not shown).

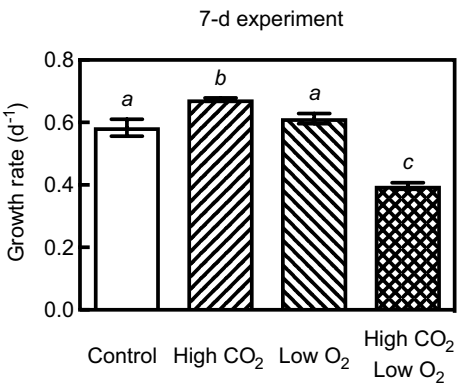

Fig. 1 *Amphidinium carterae* growth rates during 7-day incubation (mean ± SEM; $n = 4$ for all treatments), calculated from exponential increases in cell counts over the last 3 days. Different letters indicate statistical significance compared to the other treatments (one-way ANOVA with Fisher's LSD multiple comparisons, $p < 0.05$)

Table 2 Synergistic responses of *Amphidinium carterae* in the long-term (7 days) and short-term (6 h) experiments

Response	Synergistic	References
Long-term experiment (following acclimation)		
Growth	Yes	Figure 1
Dark respiration	No	Figure 2a
Gross photosynthesis	Yes	Figure 2b
Net photosynthesis	Yes	Figure 2c
^{13}C uptake	Yes	Figure 3a
^{15}N uptake	Yes	Figure 3b
RuBisCO content	No	Figure 4
F_v/F_m	Yes	Figure 5a
Short-term experiment examining metabolism		
Dark respiration	No	Figure 2d
Gross photosynthesis	No	Figure 2e
Net photosynthesis	No	Figure 2f
F_v/F_m	Yes	Figure 5b

Combined high CO_2, low O_2 conditions also had negative effects on *A. carterae* metabolism (Fig. 2). Although dark respiration rates were not significantly different among treatments (one-way ANOVA), post hoc tests indicated that combined high CO_2, low O_2 conditions significantly decreased rates of dark respiration relative to the control (Fisher's LSD multiple comparison, $p = 0.0084$; Fig. 2a), even though these responses were not synergistic (Table 2). In addition, both gross [one-way ANOVA, $F(3,8) = 48.47$, $p < 0.0001$] and net [$F(3,8) = 66.15$, $p < 0.0001$] photosynthesis rates were significantly different among treatments. Rates of gross and net photosynthesis decreased relative to the control under low O_2 conditions alone (Fisher's LSD multiple comparisons, $p = 0.0157$ and 0.0392, respectively), but the effects became synergistically negative in combination with high CO_2 conditions ($p < 0.0001$; Fig. 2b, c, Table 2). Gross and net photosynthesis rates were not significantly different between the control and high CO_2 treatments despite the significantly different growth rates described above. Relative differences in dark respiration, gross photosynthesis, and net photosynthesis rates calculated per unit RuBisCO were consistent with those calculated per cell (data not shown).

Synergistic, negative effects were also observed for qualitative measures of both ^{13}C-carbon fixation and ^{15}N-nitrate uptake following the 3-h labeling incubation under high CO_2, low O_2 conditions (Fig. 3, Table 2), which is internally consistent with the low growth and photosynthesis rates observed independently under these treatment

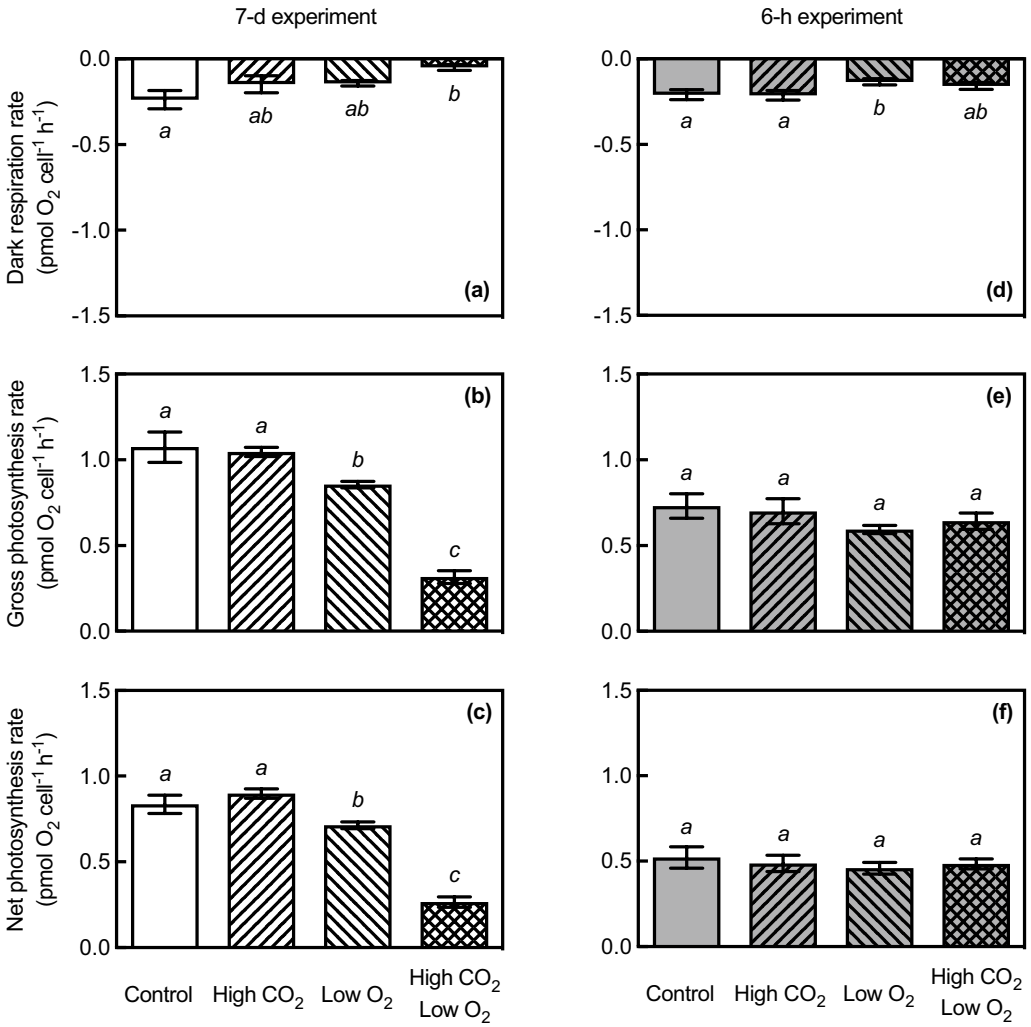

Fig. 2 Rates of *Amphidinium carterae* dark respiration, gross photosynthesis, and net photosynthesis per cell **a**–**c** after 7-day (mean ± SEM; $n = 4$ for all treatments) and **d**–**f** 6-h incubations ($n = 3$ for all treatments), calculated from changes in O_2 evolution over 5 h. Different letters indicate statistical significance compared to the other treatments in the same panel (one-way ANOVA with Fisher's LSD multiple comparisons, $p < 0.05$)

conditions. Both carbon fixation and nitrate uptake were significantly different among treatments [one-way ANOVA, $F(3,12) = 211.5$, $p < 0.0001$ and $F(3,12) = 307.3$, $p < 0.0001$, respectively]. High CO_2 and low O_2 conditions together had synergistically negative effects on ^{13}C-carbon fixation (Fisher's LSD multiple comparison, $p < 0.0001$; Fig. 3a). Separately, high CO_2 and low O_2 conditions increased ^{15}N-nitrate uptake ($p = 0.0014$ and 0.0006, respectively; Fig. 3b), but the combination synergistically decreased uptake ($p < 0.0001$).

Treatment conditions significantly affected both extracted chlorophyll *a* per cell (Fig. S3a) and protein per cell (Fig. S3b) at the end of the incubation [one-way ANOVAs, $F(3,12) = 28.4$, $p < 0.0001$ and $F(3,12) = 5.644$, $p = 0.0120$, respectively]. Compared to the control, chlorophyll per cell increased under all treatment conditions: high CO_2 (Fisher's LSD multiple comparison, $p = 0.0430$), low O_2 ($p < 0.0001$), and combined high CO_2, low O_2 conditions ($p = 0.0125$). Despite these increases in extracted chlorophyll *a* among treatments, growth rates calculated from changes of in vivo chlorophyll *a* over time (data not shown) were consistent with those based on cell counts (Fig. 1). Conversely, protein per cell decreased significantly in all treatments relative to the control: high CO_2 ($p = 0.0033$), low O_2 ($p = 0.0130$), and combined high CO_2, low O_2 ($p = 0.0059$). Although RuBisCO content as a percent of total protein was not significantly different among treatments (one-way ANOVA), post hoc tests indicated that combined high CO_2, low O_2 conditions significantly increased *A. carterae* RuBisCO content (Fisher's LSD multiple comparison, $p = 0.0373$; Fig. 4) despite decreased growth rates, albeit not synergistically (Table 2). Absolute differences in RuBisCO per cell were consistent with differences in RuBisCO content as a

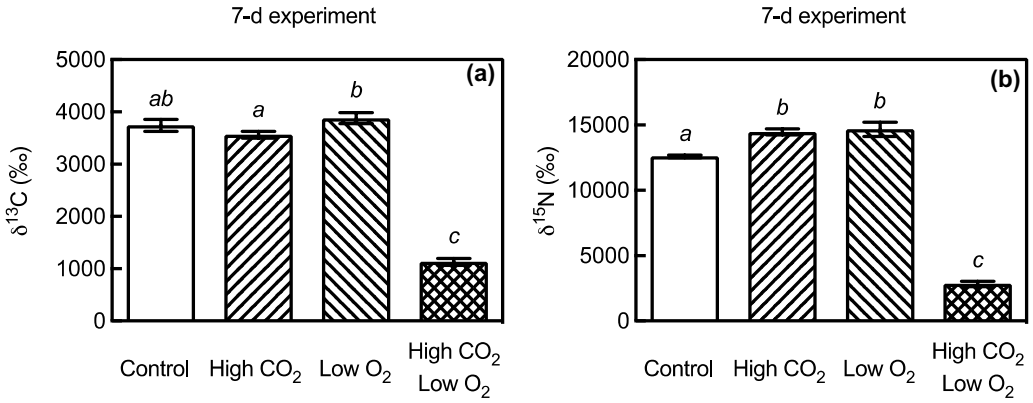

Fig. 3 Enriched **a** $\delta^{13}C$ signatures and **b** $\delta^{15}N$ signatures of *Amphidinium carterae* cells after 7-day incubation, measured after an additional 3-h ^{13}C- and ^{15}N-labeling incubation (mean ± SEM; $n = 4$ for all treatments). Notes that these signatures are a qualitative index of carbon fixation and nitrate uptake, respectively. Different letters indicate statistical significance compared to the other treatments in the same panel (one-way ANOVA with Fisher's LSD multiple comparisons, $p < 0.05$)

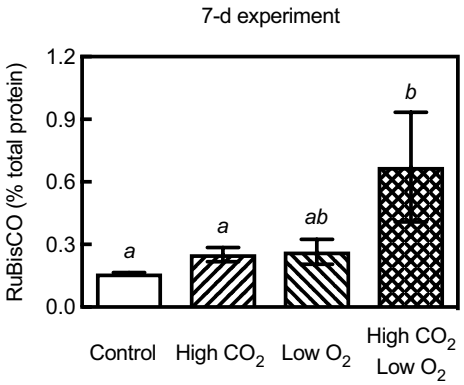

Fig. 4 RuBisCO content in *Amphidinium carterae* cells after 7-day incubation (mean ± SEM; $n = 4$ for all treatments). Different letters indicate statistical significance compared to the other treatments (one-way ANOVA with Fisher's LSD multiple comparisons, $p < 0.05$)

percent of total protein (Fig. S3c), so the effect of increasing RuBisCO was not simply a denominator effect (e.g., caused by low protein per cell).

High CO_2 and low O_2 treatment conditions also caused synergistic, negative effects on F_v/F_m [one-way ANOVA, $F(3,12) = 118.2$, $p < 0.0001$; Fig. 5a, Table 2]. At the end of the 7-day incubation, F_v/F_m significantly decreased in the high CO_2, low O_2 treatment (Fisher's LSD multiple comparison, $p < 0.0001$), and to a lesser extent, in the high CO_2 ($p = 0.0310$) and low O_2 treatments ($p = 0.0001$).

Short-term impacts on metabolism

Cell counts and in vivo chlorophyll *a* measurements at the beginning of the 6-h incubation were within the range of values measured the end of the long-term experiment (data not

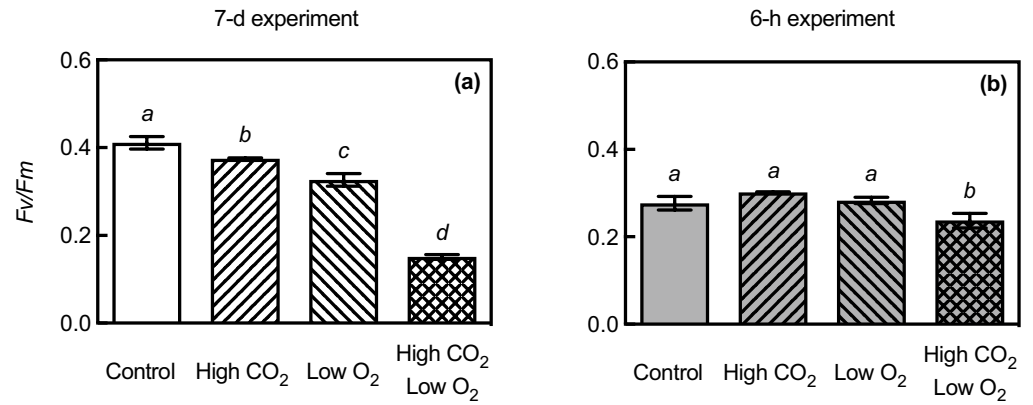

Fig. 5 Maximum quantum yield of photosystem II (*Fv/Fm*) in *Amphidinium carterae* cells after **a** 7-day (mean ± SEM; n = 4 for all treatments) and **b** 6-h incubations ($n = 4$ for all treatments). Different letters indicate statistical significance compared to the other treatments in the same panel (one-way ANOVA with Fisher's LSD multiple comparisons, $p < 0.05$)

shown). Measurements of O_2 and pH_T were also comparable to those in the long-term experiment (Table 1).

A. carterae metabolism was affected little by the treatment conditions over 6-h exposure. Linear regressions of oxygen concentrations over time were used to estimate dark respiration (linear regressions from all treatments, $R^2 > 0.9290$), gross photosynthesis ($R^2 > 0.9588$), and net photosynthesis rates ($R^2 > 0.9458$). Although respiration rates over the course of the short-term incubation were negatively impacted at low O_2 (Fisher's LSD multiple comparison, $p = 0.0489$; Fig. 2d), combined high CO_2, low O_2 conditions did not significantly affect respiration or photosynthesis rates (one-way ANOVA; Fig. 2d–f). Therefore, the synergistic effects of CO_2 and O_2 on *A. carterae* metabolism described above (and summarized in Table 2) were not immediate and rather developed over time.

Although F_v/F_m did not initially differ significantly among treatments (data not shown), F_v/F_m was significantly impacted under treatment conditions after 6-h exposure [one-way ANOVA, $F(3,12) = 5.204$, $p = 0.0156$; Fig. 5b]. Combined high CO_2, low O_2 treatment conditions significantly decreased F_v/F_m relative to the control (Fisher's LSD multiple comparison, $p = 0.0362$). This decrease in F_v/F_m was largely driven by decreases in F_m (data not shown), indicating a greater number of closed PSII reaction centers (Ulstrup et al. 2005).

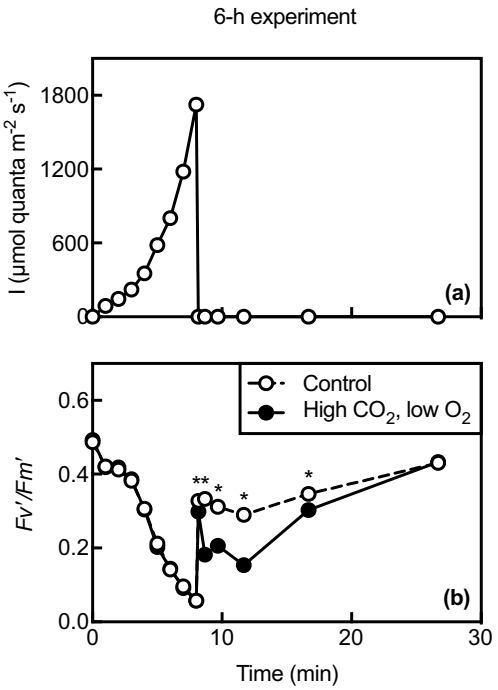

Fig. 6 Induction-recovery curves after 6-h incubation including **a** actinic light irradiance levels (I) and **b** the resulting effective quantum yield of photosystem II (F_v'/F_m') of *Amphidinium carterae* cells (mean ± SEM; $n = 3$ for both treatments). The asterisk indicates statistical significance between treatments at a particular time point (two-way ANOVA with Fisher's LSD multiple comparisons, $p < 0.05$)

Short-term impacts on photophysiology

Photophysiology of *A. carterae* was also affected following 6-h incubation, as demonstrated by the light curves with dark recovery (Fig. 6). Experimental cultures in this experiment contained higher biomass (cell counts and chlorophyll *a*) than those in the other experiments to improve signal strength on the PAM unit (data not shown). Nevertheless, O_2 and pH_T values were similar to those in the other experiments (Table 1). Relative differences in initial and final F_v/F_m measurements were consistent with the findings from the previous short-term experiment (data not shown). Under increasing actinic light intensities (Fig. 6a), F_v'/F_m' was not significantly different between the control and the combined high CO_2, low O_2 treatments (Fig. 6b). Similarly, during actinic irradiation, relative ETR was not significantly different between those two treatments (Fig. S4). During the period of recovery following actinic irradiation, however, F_v'/F_m' remained significantly lower under high CO_2, low O_2 conditions compared to the control [two-way ANOVA, $F(14,56) = 31.36$, $p < 0.0001$; Fig. 6b] for ~ 10 min, indicating delayed recovery of PSII reaction centers following photoinhibition and potentially suppressed repair of PSII (Takahashi et al. 2007). In addition, during the first ~ 10 min of recovery, NPQ was consistently higher in the combined high CO_2, low O_2 treatment relative to the control (Fig. S5), but this trend was not significant.

Discussion

Synergistic, negative responses to acidification and hypoxia

In the long-term experiment, synergistically negative effects were consistently observed for *Amphidinium carterae* under combined high CO_2, low O_2 conditions. Contrary to expectations based on low in vitro RuBisCO specificity, these conditions negatively affected *A. carterae* growth, dark respiration, gross and net photosynthesis, carbon fixation and nitrate uptake, F_v/F_m, and cellular RuBisCO content. In general, there were relatively small (though sometimes statistically significant) differences among the control, high CO_2, and low O_2 treatments, but very large differences (~ 40 to 60%) between the control and high CO_2, low O_2 treatments. Most of these differences between the control and high CO_2, low O_2 treatments could be described as synergistic, insofar as the effects of the combined stressors were larger than the additive effects of either high CO_2 or low O_2

by themselves. Not only were these responses to combined high CO_2, low O_2 conditions often synergistic, they were surprising (i.e., responses often opposed those under high CO_2 or low O_2 conditions alone). It should be noted that many of these measurements were quantified using fully independent methods and that any potential confounding impacts related to changes in temperature, irradiance, or macronutrient concentrations can also be excluded.

In the short-term experiments, high CO_2 and low O_2 conditions negatively affected photosynthesis in *A. carterae* even after relatively short exposures. In comparison to the long-term experiment, any differences between the control and high CO_2, low O_2 treatments in the short-term experiments were muted. Nevertheless, these patterns showed that *A. carterae* responses to combined acidification and hypoxia were rapid, with changes in physiology becoming apparent within 6 h of exposure. In addition, the temporal progression from relatively minor impacts of F_v/F_m after several hours to major impacts on multiple photosynthetic and metabolic pathways after several days of continuous exposure suggests that impacts were cumulative over time. Such a temporal progression is less consistent with a simple direct pathway (e.g., direct kinetics effects on RuBisCO) and more consistent with a complex pathway (e.g., multiple changing physiological processes or damage to one or more subcellular components over time). It is important to consider these temporal changes when considering possible explanations for the observed effects of *A. carterae* under combined high CO_2, low O_2 conditions and when comparing the results of this study to other related work.

Prior studies examining effects of CO_2 and/or O_2

Results from some of the numerous prior studies that documented the effects of CO_2 and/or O_2 on photosynthetic organisms are summarized in Table 3. While a comprehensive review would be outside the scope of this study, Table 3 is sufficient to demonstrate several key points. First, combined manipulations of CO_2 and O_2—especially over long durations—are rare, which is unfortunate, because these gases are often functionally linked in aquatic environments. To predict the potential for synergistic impacts of CO_2 and O_2 on a given photosynthetic organism (as shown in this study), both gases must be simultaneously varied; simply adding together the effects of each gas individually may be very misleading. Second, the responses of different photosynthetic organisms to changes in CO_2 and/or O_2 are not consistent. While some of this variability may be related to methodological differences between studies (e.g., hypoxic versus anoxic medium; the degree of CO_2 elevation; the method used to acidify the culture medium), enough of the studies are sufficiently similar to show that even organisms belonging to related taxa may respond differently to a given CO_2 or O_2 treatment. Even responses to elevated CO_2 alone have been previously shown to be species-specific (e.g., Young et al. 2015b). For example, different species of the dinoflagellate genus, *Alexandrium*, have been shown to either increase growth, decrease growth, or remain unaffected under high CO_2 (e.g., Eberlein et al. 2014; Hattenrath-Lehmann et al. 2015; Hennon et al. 2017). Some of this species-specificity may be caused by the many, distinct pathways for optimizing photosynthesis available to photosynthetic organisms in response to changing CO_2 and O_2 concentrations (as described below).

Despite the fact that physiological effects to changing CO_2 and O_2 conditions depend on both methodology and the species tested, the major finding of this study—the synergistic, negative effects of combined high CO_2, low O_2 on A. carterae—is not without precedent. Bagby and Chisholm (2015) measured growth and chlorophyll fluorescence in the open-ocean cyanobacterium, *Prochlorococcus* (strain MED4), under a range of CO_2 and O_2 conditions. *Prochlorococcus* growth and chlorophyll fluorescence per cell decreased under low CO_2 concentrations (~ 40 ppmv; presumably due to CO_2 limitation of photosynthesis) and markedly decreased under ~ atmospheric CO_2 (360 ppmv) and very low O_2 (0.001%) conditions (presumably due to photodamage under non-photorespiratory conditions). The decline in chlorophyll fluorescence was detectable within 1–2 days, while the effect on growth rate accumulated over the course of the 4-day exposure. Given the similarity between the results of Bagby and Chisholm (2015) and those of this study (i.e., decreased growth under non-photorespiratory conditions), it is worth noting that both cyanobacteria and dinoflagellates have similarly low RuBisCO specificities compared to other phytoplankton groups (Whitney and Andrews 1998; Tortell 2000).

In another related study, Kitaya et al. (2008) measured growth of the symbiotic dinoflagellate, *Amphidinium* sp. (isolated from the flatworm *Amphiscolops* sp.), under different CO_2 and O_2 conditions. Growth rates changed little under a range of CO_2 (20–1000 ppmv) and O_2 (0.2–21%) conditions over continuous 6-day incubation, but decreased significantly (~ 50%) under combined 'low' O_2 (5%) and 'high' bicarbonate (10 mM) concentrations. Thus, Kitaya et al. (2008) described a similar negative synergy to that observed in this study under high CO_2, low O_2 conditions, albeit likely at a higher dissolved inorganic carbon (DIC) concentration. However, it is important to note several key differences between the methodologies of Kitaya et al. (2008) and this study. First, since Kitaya et al. (2008) used higher O_2 concentrations than those in our 'low O_2' treatments, ambient CO_2:O_2 ratios were likely very different. Second, their bicarbonate additions would have changed the carbonate chemistry of the medium (e.g., increased A_T and DIC; Riebesell et al. 2011), but to what extent is unknown.

Table 3 Previous studies examining organismal responses to CO_2 and O_2, both individually and in combination

	Organism	High CO_2 (or low pH)	Low O_2	High CO_2, low O_2	References
Long-term experiments (≥ 1 day)					
Growth					
Dinophytes	*Amphidinium carterae*	↑	↔	↓	This study
	Amphidinium sp.	↔	↔	↔, ↓[a]	Kitaya et al. (2008)
	Alexandrium fundyense	↑			Hattenrath-Lehmann et al. (2015)
	Alexandrium monilatum	↓			Hennon et al. (2017)
	Alexandrium tamarense	↔			Eberlein et al. (2014)
	Cochlodinium polykrikoides	↔			Bausch et al. (2017)
	Karlodinium veneficum	↑[b]			Fu et al. (2012)
	Prorocentrum minimum	↔			Fu et al. (2008)
	Prorocentrum minimum	↔[b]			Fu et al. (2012)
	Prorocentrum minimum	↓			Hennon et al. (2017)
	Scrippsiella trochoidea	↔			Eberlein et al. (2014)
Bacillariophytes	Antarctic community	↔			Young et al. (2015b)
	Chaetoceros affinis	↔			Hennon et al. (2017)
	Phaeodactylum tricornutum	↓			Laws et al. (1997)
	Phaeodactylum tricornutum	↑			Wu et al. (2010)
	Phaeodactylum tricornutum	↑↓			Liu et al. (2017)
	Skeletonema costatum		↓		Wu et al. (2012)
	Thalassiosira pseudonana	↑			Sobrino et al. (2008)
Chlorophytes	*Chlamydomonas reinhardtii*		↓		Godaux et al. (2015)
Raphidophytes	*Chattonella subsalsa*	↑			Fu et al. (2012)
	Heterosigma akashiwo	↑			Fu et al. (2008)
	Heterosigma akashiwo	↑			Hennon et al. (2017)
Haptophytes	*Chrysochromulina polylepis*	↑			Hennon et al. (2017)
	Gephyrocapsa oceanica	↔			Hennon et al. (2017)
Cyanobacteria	*Prochlorococcus*	↑	↓	↓	Bagby and Chisholm (2015)
Aquatic plants	*Salvinia natans*		↓		Jampeetong and Brix (2009)
Net photosynthesis					
Dinophytes	*Amphidinium carterae*	↔	↓	↓	This study
	Alexandrium tamarense	↓			Eberlein et al. (2014)
	Scrippsiella trochoidea	↔			Eberlein et al. (2014)
	Symbiodinium sp.	↓			Crawley et al. (2010)
Bacillariophytes	*Phaeodactylum tricornutum*	↑↓			Burns and Beardall (1987)
	Phaeodactylum tricornutum	↑			Wu et al. (2010)
	Phaeodactylum tricornutum	↔↓			Liu et al. (2017)
	Thalassiosira pseudonana	↑			Sobrino et al. (2008)
Rhodophytes	*Porphyridium purpureum*	↑			Burns and Beardall (1987)
Cyanobacteria	*Oscillatoria woronichinii*	↑			Burns and Beardall (1987)
Macroalgae	*Cladophora vagabunda*		↓		Peckol and Rivers (1995)
	Reef flat community		↑		Gruber et al. (2017)
Seagrasses	Reef flat community		↑		Gruber et al. (2017)
Dark respiration					
Dinophytes	*Amphidinium carterae*	↔	↔	↓	This study
	Alexandrium tamarense	↑			Eberlein et al. (2014)
	Scrippsiella trochoidea	↔			Eberlein et al. (2014)
	Symbiodinium sp.	↔			Crawley et al. (2010)
Bacillariophytes	*Phaeodactylum tricornutum*	↑			Wu et al. (2010)
Macroalgae	Reef flat community		↓		Gruber et al. (2017)

Table 3 (continued)

	Organism	High CO_2 (or low pH)	Low O_2	High CO_2, low O_2	References
Seagrasses	Reef flat community		↓		Gruber et al. (2017)
Land plants	*Glycine max*	↓			Gonzàlez-Meler et al. (1996)
	Lindera benzoin	↓			Azcón-Bieto et al. (1994)
	Scirpus olneyi	↓			Azcón-Bieto et al. (1994)
	Spartina patens	↔			Azcón-Bieto et al. (1994)
	Xanthium strumarium	↓			Tcherkez et al. (2008)
Photorespiration					
Dinophytes	*Alexandrium monilatum*	↓[c]			Hennon et al. (2017)
	Prorocentrum minimum	↓[c]			Hennon et al. (2017)
	Symbiodinium sp.	↓[c]			Crawley et al. (2010)
Bacillariophytes	*Chaetoceros affinis*	↔[c]			Hennon et al. (2017)
Raphidophytes	*Heterosigma akashiwo*	↑[c]			Hennon et al. (2017)
Haptophytes	*Chrysochromulina polylepis*	↑[c]			Hennon et al. (2017)
	Gephyrocapsa oceanica	↔[c]			Hennon et al. (2017)
F_v/F_m					
Dinophytes	*Amphidinium carterae*	↓	↓	↓	This study
	Prorocentrum minimum	↔			Fu et al. (2008)
	Symbiodinium sp.		↓		Ulstrup et al. (2005)
Bacillariophytes	*Phaeodactylum tricornutum*	↔			Liu et al. (2017)
	Thalassiosira pseudonana	↔			Sobrino et al. (2008)
Raphidophytes	*Heterosigma akashiwo*	↔			Fu et al. (2008)
Aquatic plants	*Salvinia natans*		↓		Jampeetong and Brix (2009)
ETR					
Dinophytes	*Symbiodinium* sp.		↓		Roberty et al. (2014)
Bacillariophytes	*Phaeodactylum tricornutum*	↓			Wu et al. (2010)
	Phaeodactylum tricornutum	↑			Liu et al. (2017)
Aquatic plants	*Salvinia natans*		↓		Jampeetong and Brix (2009)
Short-term experiments (< 1 day)					
Growth					
Bacillariophytes	*Phaeodactylum tricornutum*			↔[a]	Pope (1975)
	Thalassiosira weissflogii	↔			Goldman et al. (2017)
Cyanobacteria	*Anacystis nidulans*			↑[a]	Pope (1975)
Net photosynthesis					
Dinophytes	*Amphidinium carterae*	↔	↔	↔	This study
Bacillariophytes	*Chaetoceros* sp.		↔		Bunt (1971)
	Cocconeis diminuta		↔		Bunt (1971)
	Fragilaria sublinearis		↓		Bunt (1971)
	Navicula pelliculosa		↔		Birmingham et al. (1982)
	Phaeodactylum tricornutum		↑		Pope (1975)
	Thalassiosira weissflogii	↔			Goldman et al. (2017)
Chlorophytes	*Chlamydomonas reinhardtii*		↔		Birmingham et al. (1982)
	Chlamydomonas reinhardtii	↑			Peltier and Thibault (1983)
	Chlamydomonas sp.		↔		Bunt (1971)
	Chlorella vulgaris		↔		Birmingham et al. (1982)
	Dunaliella tertiolecta		↑		Bunt (1971)
	Dunaliella tertiolecta		↑		Pope (1975)
	Unidentified species		↑		Bunt (1971)
Haptophytes	*Cricosphaera* sp.		↔		Pope (1975)

Table 3 (continued)

	Organism	High CO_2 (or low pH)	Low O_2	High CO_2, low O_2	References
Cyanobacteria	*Anabaena flos-aquae*		↔		Birmingham et al. (1982)
	Anacystis nidulans		↑		Pope (1975)
	Anacystis nidulans		↔		Birmingham et al. (1982)
	Coccochloris peniocystis		↔		Birmingham et al. (1982)
	Phormidium molle		↔		Birmingham et al. (1982)
Dark respiration					
Dinophytes	*Amphidinium carterae*	↔	↓	↔	This study
Bacillariophytes	*Thalassiosira weissflogii*	↔			Goldman et al. (2017)
Macroalgae	*Cladophora vagabunda*		↔		Peckol and Rivers (1995)
	Gracilaria tikvahiae		↓		Peckol and Rivers (1995)
Photorespiration					
Bacillariophytes	*Navicula pelliculosa*		↓		Birmingham et al. (1982)
Chlorophytes	*Chlamydomonas reinhardtii*		↓		Birmingham et al. (1982)
	Chlamydomonas reinhardtii	↓	↓		Peltier and Thibault (1983)
	Chlorella vulgaris		↓		Birmingham et al. (1982)
Cyanobacteria	*Anabaena flos-aquae*		↓		Birmingham et al. (1982)
	Anacystis nidulans		↓		Birmingham et al. (1982)
	Coccochloris peniocystis		↔		Birmingham et al. (1982)
	Phormidium molle		↔		Birmingham et al. (1982)
F_v/F_m					
Dinophytes	*Amphidinium carterae*	↔	↔	↓	This study
	Symbiodinium sp.		↓		Jones and Hoegh-Guldberg (2001)
Bacillariophytes	*Thalassiosira pseudonana*	↓			Sobrino et al. (2008)
Land plants	*Quercus ilex*		↓		Peñuelas and Llusià (2002)
ETR					
Dinophytes	*Amphidinium carterae*			↔	This study
Chlorophytes	*Chlamydomonas reinhardtii*		↓		Finazzi et al. (1999)
	Chlamydomonas reinhardtii		↓		Godaux et al. (2015)
	Scenedesmus obliquus		↓		Schreiber and Vidaver (1974)
Land plants	*Quercus ilex*		↓		Peñuelas and Llusià (2002)

The ↑, ↓, and ↔ symbols indicate an increase, a decrease, or no change in response to treatment conditions, respectively. Values of 'high' CO_2 or 'low' O_2 are relative within a given study. Note that this list is not exhaustive

[a]Following HCO_3^- additions

[b]In an interspecific competition experiment

[c]Based on gene expression

Third, the isolate used in Kitaya et al. (2008), although congeneric with the *A. carterae* strain used in this study, was isolated from an animal symbiosis. Symbiotic algae may have developed very different physiologies to adapt to the challenges of living inside another organism. Furthermore, animal tissues may have significantly different carbonate chemistry and/or O_2 concentrations than their external environment (e.g., Jones and Hoegh-Guldberg 2001; Crawley et al. 2010).

The slight but significant increase in *A. carterae* growth in the high CO_2 treatment is consistent with some previous research, which suggested that *A. carterae* growth may be stimulated under elevated CO_2 due to a lack of external CA and, therefore, a potentially limited capacity for direct bicarbonate uptake (Dason et al. 2004; Fu et al. 2012). It is important to note, however, that there is evidence of a CCM in *A. carterae* (Burns and Beardall 1987; Leggat et al. 1999).

The finding that low O_2 by itself did not affect *A. carterae* growth and physiology is novel in that, to the best of our knowledge, the impacts of hypoxia on free-living dinoflagellates have yet to be described in the literature. Although some algae can be successfully cultivated under light/dark-anoxic cycles (e.g., *Chlamydomonas reinhardtii*; Godaux et al. 2015), many photosynthetic organisms have negative

responses to low O_2 conditions (Table 3). Among the dinoflagellate symbionts of corals (*Symbiodinium* sp.), low O_2 conditions have been shown to decrease ETR, close PSII reaction centers, decrease F_m, and ultimately decrease F_v/F_m (Jones and Hoegh-Guldberg 2001; Ulstrup et al. 2005; Roberty et al. 2014). However, as mentioned above, it is difficult to predict the relevance of the physiological responses of symbiotic organisms for free-living algae.

Our initial expectation was that *A. carterae* growth and physiology would benefit under combined high CO_2, low O_2 conditions, given that these conditions should maximize carbon fixation and minimize photorespiration (Foyer and Noctor 2000; Tortell 2000), especially in an organism with such a low RuBisCO substrate specificity (Whitney and Andrews 1998). Although our findings refuted this initial hypothesis, the impacts of combined acidification and hypoxia on multiple photosynthetic parameters and RuBisCO content strongly indicated that the mechanism driving these impacts was related to organismal regulation of photophysiology. Direct and indirect effects of high CO_2, low O_2 conditions on other aspects of *A. carterae* physiology are certainly likely, but we restrict our discussion to photophysiological mechanisms.

Photosynthetic redox poise

One possible explanation for the interactive effects of CO_2 and O_2 on *A. carterae* involves the 'redox poise', the balance between the oxidized and reduced components of the photosynthetic electron transport chain (Finazzi et al. 2010). Redox poise can be regulated by decreasing photon capture (often resulting in high NPQ; e.g., Brooks and Niyogi 2011) and through several alternate electron pathways (AEPs), such as cyclic electron flow around photosystem I (PSI), photorespiration, and several oxygen-dependent pathways such as the Mehler reaction, chlororespiration, and mitochondrial respiration (Behrenfeld et al. 2008; Finazzi et al. 2010; Cardol et al. 2011). The findings in this study are consistent with over-reduced photosynthetic redox poise under high CO_2 low O_2 conditions. Specifically, observed changes in F_v/F_m are related to redox poise (e.g., due to non-photochemical reduction of the plastoquinone pool). In the long-term experiment, decreased F_v/F_m suggests that there were excess electrons in linear photosynthetic electron flow despite the subsaturating light levels used. In the short-term experiment, the ETR and NPQ values were similar in the high CO_2, low O_2 and control treatments, indicating that the initial electron flux from PSII was essentially identical in both treatments. Over-reduced redox poise in the high CO_2, low O_2 treatment could have developed downstream of PSII if treatment conditions inhibited one or more AEPs that were needed to regulate electron flow from PSII. All of the oxygen-dependent AEPs mentioned above could be inhibited under low O_2 conditions, but only photorespiration would likely be particularly sensitive to CO_2:O_2 ratios. In this study, photorespiration likely decreased significantly in the high CO_2, low O_2 treatment (e.g., Birmingham et al. 1982; Peltier and Thibault 1983). While these non-photorespiratory conditions should have increased RuBisCO carbon fixation efficiency, they may also have caused over-reduced redox poise, decreased photosynthetic efficiency, and/or eventual damage to subcellular components (Foyer and Noctor 2000; Bauwe et al. 2012; Bagby and Chisholm 2015).

Non-photorespiratory conditions have been described as potentially damaging, particularly under high light regimes (e.g., Hackenberg et al. 2009). However, Bagby and Chisholm (2015) found that gene expression responses in the cyanobacterium, *Prochlorococcus*, under a high CO_2:O_2 ratio resembled those under high light stress, indicating that non-photorespiratory conditions may cause a 'photosynthetic impedance mismatch'—defined as resistance in dissipating excess light energy—even under moderate light conditions. Similarly, Crawley et al. (2010) showed that the expression of phosphoglycolate phosphatase (PGPase)—the first enzyme in the photorespiration pathway—in the symbiotic dinoflagellate, *Symbiodinium* sp., decreased under high CO_2 conditions, even though the light conditions were subsaturating. The concept that photorespiration is a beneficial (e.g., photoprotective), possibly even essential, physiological process under stress conditions has been described for many photosynthetic organisms (e.g., Takahashi et al. 2007; Hackenberg et al. 2009; Bagby and Chisholm 2015). Therefore, if photorespiration serves an important stress response and regulatory role in *A. carterae* (rather than simply diverting from carbon fixation), the non-photorespiratory conditions under combined high CO_2 and low O_2 could lead to poor cellular performance, even though RuBisCO itself might be more efficient. In addition to photorespiration, inhibition of oxygen-dependent AEPs under low O_2 conditions could also have contributed to an imbalance in the redox poise of *A. carterae*.

RuBisCO activase

One alternative—or additional—explanation for the synergistic responses of *A. carterae* in the high CO_2, low O_2 treatment could involve RuBisCO activase. Various substrates can inhibit RuBisCO by binding to its active site (Parry et al. 2008). Activation of RuBisCO (i.e., the release of these substrates to allow for the binding of CO_2) requires RuBisCO activase, which, in land plants, is inhibited under high CO_2, low O_2 conditions (Crafts-Brandner and Salvucci 2000). However, the RuBisCO activases of dinoflagellates are likely highly divergent from those of the green plastid lineage (Loganathan et al. 2016), and their responses to CO_2 and O_2 concentrations have not been documented.

Changes in RuBisCO content

While the RuBisCO content measured in this study (< 1% total protein) was within the range of values measured in some natural phytoplankton populations (Losh et al. 2013), the increase in RuBisCO content in the combined high CO_2, low O_2 treatment was unexpected. High CO_2 conditions have been generally shown to decrease RuBisCO content among land plants and algae (e.g., Losh et al. 2013; Raven 2013), but not in the dinoflagellate *Protoceratium reticulatum* (Pierangelini et al. 2017). It seems surprising that the *A. carterae* in this study would produce more RuBisCO if the light reactions were impaired, RuBisCO activase was potentially inhibited, and cells fixed less CO_2. It is possible, however, that the *A. carterae* cells increased their RuBisCO content to compensate for photosynthetic impairment, as described above (e.g., redox imbalances and slow RuBisCO activase kinetics). Such compensatory changes in RuBisCO content are consistent with several previous studies of diatoms and chlorophytes showing increased resource allocation to RuBisCO under stress conditions including low nitrogen (Li and Campbell 2017) and low temperature (Devos et al. 1998; Losh et al. 2013; Young et al. 2015a).

Changes in CCM activity

It is important to note the potential effects of the experimental conditions on the CCM of *A. carterae*. High CO_2 conditions have been shown to decrease CCM activity in the dinoflagellate *P. reticulatum* (Ratti et al. 2007). It is possible that the CCM activity of *A. carterae*, however limited (Dason et al. 2004), could decrease at a high CO_2:O_2 ratio and subsequently impact organismal photophysiology.

Future prospects and conclusions

The experimental results of this study demonstrate strong, synergistic interactions between CO_2 and O_2 availability in a toxic dinoflagellate. Additional experiments under a broad range of CO_2:O_2 ratios, possibly using chemical inhibitors of AEPs or AEP-deficient mutant cell lines, are required to better understand the role of AEPs on the growth and physiology of *A. carterae*. In addition, other free-living dinoflagellates need to be examined to determine the generality of our findings for *A. carterae*. Future work should include both long-term and short-term exposures to changing CO_2 and O_2 conditions. In addition, the extent of oxidative damage to phytoplankton cells and the possible beneficial role of AEPs in avoiding such damage need to be assessed under a wide range of light, CO_2, and O_2 conditions. Because interactive effects of ocean acidification with other environmental drivers are often surprising (e.g., Bausch et al. 2017), we caution that predicting physiological synergies within any phytoplankton species is difficult—if not impossible—without performing empirical studies. We also suggest that combined coastal acidification and hypoxia may have negative, synergistic impacts on the growth, metabolism, and physiology of some phytoplankton in coastal ecosystems over the course of this century, as shown in the case of *A. carterae*. These findings may help to improve understanding of the effects of multi-stressors on an organismal level in coastal ecosystems, as well as the broader impacts of future anthropogenic climate change on the base of the food web in zones of both acidification and hypoxia.

Acknowledgements The authors would like to thank Sonya Dyhrman and Sheean Haley at Lamont-Doherty Earth Observatory (LDEO) for providing laboratory space and logistical support; Hugh Ducklow, Robert Anderson, Kevin Griffin, and Gwenn Hennon at LDEO, Christopher Hayes at the University of Southern Mississippi, and the Editor and Reviewer for providing feedback on the manuscript; Wei Huang at LDEO for performing the isotopic analyses; Jerry Frank at the Chesapeake Biological Laboratory for performing the nutrient analyses; Andrew Dickson at Scripps Institution of Oceanography for providing the CO_2 seawater reference materials; and Naomi Shelton and Clara Chang at LDEO for providing laboratory assistance. This is contribution #8317 from Lamont–Doherty Earth Observatory.

Funding This work was partly supported by NASA Headquarters under the NASA Earth and Space Science Fellowship Program grant 15-EARTH15R-5. Funding was also provided by the Natural Sciences and Engineering Research Council of Canada and the Chevron Student Initiative Fund from the Department of Earth and Environmental Sciences at Columbia University.

Compliance with ethical standards

Conflict of interest The authors Alexandra Bausch, Andrew Juhl, and Natalie Donaher declare no conflicts of interest. The author Amanda Cockshutt declares a potential financial interest as part owner of Environmental Proteomics NB Inc., an Agrisera business partner.

Human and animal rights statement All authors have agreed to the submitted version of this manuscript. This manuscript does not contain any studies with humans or animals performed by any of the authors.

References

Azcón-Bieto J, Gonzàlez-Meler MA, Doherty W, Drake BG (1994) Acclimation of respiratory O_2 uptake in green tissues of field-grown native species after long-term exposure to elevated atmospheric CO_2. Plant Physiol 106(3):1163–1168. https://doi.org/10.1104/pp.106.3.1163

Badger MR, Andrews TJ, Whitney SM, Ludwig M et al (1998) The diversity and coevolution of RuBisCO, plastids, pyrenoids, and chloroplast-based CO_2-concentrating mechanisms in algae. Can J Bot 76(6):1052–1071. https://doi.org/10.1139/cjb-76-6-1052

Bagby SC, Chisholm SW (2015) Response of *Prochlorococcus* to varying CO_2:O_2 ratios. Int Soc Microb Ecol 9(10):2232–2245. https://doi.org/10.1038/ismej.2015.36

Baumann H (2016) Combined effects of ocean acidification, warming, and hypoxia on marine organisms. Limnol Oceanogr e-Lect 6(1):1–43. https://doi.org/10.1002/loe2.10002

Bausch AR, Boatta F, Morton PL, McKee KT et al (2017) Elevated toxic effect of sediments on growth of the harmful dinoflagellate *Cochlodinium polykrikoides* under high CO_2. Aquat Microb Ecol 80(2):139–152. https://doi.org/10.3354/ame01848

Bauwe H, Hagemann M, Fernie AR (2010) Photorespiration: players, partners and origin. Trends Plant Sci 15(6):330–336. https://doi.org/10.1016/j.tplants.2010.03.006

Bauwe H, Hagemann M, Kern R, Timm S (2012) Photorespiration has a dual origin and manifold links to central metabolism. Curr Opin Plant Biol 15(3):269–275. https://doi.org/10.1016/j.pbi.2012.01.008

Behrenfeld MJ, Halsey KH, Milligan AJ (2008) Evolved physiological responses of phytoplankton to their integrated growth environment. Phil Trans R Soc B 363:2687–2703. https://doi.org/10.1098/rstb.2008.0019

Birmingham BC, Coleman JR, Colman B (1982) Measurement of photorespiration in algae. Plant Physiol 69(1):259–262. https://doi.org/10.1104/pp.69.1.259

Bowes G, Ogren WL, Hageman RH (1971) Phosphoglycolate production catalyzed by ribulose diphosphate carboxylase. Biochem Biophys Res Commun 45(3):716–722. https://doi.org/10.1016/0006-291X(71)90475-X

Breitburg DL, Salisbury J, Bernhard JM, Cai W-J et al (2015) And on top of all that… Coping with ocean acidification in the midst of many stressors. Oceanogr 28(2):48–61. https://doi.org/10.5670/oceanog.2015.31

Brooks MD, Niyogi KK (2011) Use of a pulse-amplitude modulated chlorophyll fluorometer to study the efficiency of photosynthesis in *Arabidopsis* plants. In: Jarvis RP (ed) Chloroplast research in Arabidopsis: methods and protocols. Springer, New York, pp 299–310

Bunt JS (1971) Levels of dissolved oxygen and carbon fixation by marine microalgae. Limnol Oceanogr 16(3):564–566. https://doi.org/10.4319/lo.1971.16.3.0564

Burns BD, Beardall J (1987) Utilization of inorganic carbon by marine microalgae. J Exp Mar Biol Ecol 107(1):75–86. https://doi.org/10.1016/0022-0981(87)90125-0

Cai W-J, Hu X, Huang W-J, Murrell MC et al (2011) Acidification of subsurface coastal waters enhanced by eutrophication. Nat Geosci 4(11):766–770. https://doi.org/10.1038/ngeo1297

Caldeira K, Wickett ME (2003) Anthropogenic carbon and ocean pH. Nature 425(6956):365. https://doi.org/10.1038/425365a

Caldeira K, Wickett ME (2005) Ocean model predictions of chemistry changes from carbon dioxide emissions to the atmosphere and ocean. J Geophys Res 110:1–12. https://doi.org/10.1029/2004JC002671

Cao C, Sun S, Wang X, Liu W, Liang Y (2011) Effects of manganese on the growth, photosystem II and SOD activity of the dinoflagellate *Amphidinium* sp. J Appl Phycol 23(6):1039–1043. https://doi.org/10.1007/s10811-010-9637-0

Cardol P, Forti G, Finazzi G (2011) Regulation of electron transport in microalgae. Biochim Biophys Acta 1807:912–918. https://doi.org/10.1016/j.bbabio.2010.12.004

Cornwall CE, Hurd CL (2016) Experimental design in ocean acidification research: problems and solutions. ICES J Mar Sci 73(3):572–581. https://doi.org/10.1093/icesjms/fsv118

Crafts-Brandner SJ, Salvucci ME (2000) RuBisCO activase constrains the photosynthetic potential of leaves at high temperature and CO_2. Proc Natl Acad Sci 97(24):13430–13435. https://doi.org/10.1073/pnas.230451497

Crawley A, Kline DI, Dunn S, Anthony K, Dove S (2010) The effect of ocean acidification on symbiont photorespiration and productivity in *Acropora formosa*. Glob Change Biol 16(2):851–863. https://doi.org/10.1111/j.1365-2486.2009.01943.x

Dason JS, Huertas IE, Colman B (2004) Source of inorganic carbon for photosynthesis in two marine dinoflagellates. J Phycol 40(2):285–292. https://doi.org/10.1111/j.1529-8817.2004.03123.x

DePasquale E, Baumann H, Gobler CJ (2015) Vulnerability of early life stage Northwest Atlantic forage fish to ocean acidification and low oxygen. Mar Ecol Prog Ser 523:145–156. https://doi.org/10.3354/meps11142

Devos N, Ingouff M, Loppes R, Matagne RF (1998) RuBisCO adaptation to low temperatures: a comparative study in psychrophilic and mesophilic unicellular algae. J Phycol 34(4):655–660. https://doi.org/10.1046/j.1529-8817.1998.340655.x

Diaz RJ, Rosenberg R (2008) Spreading dead zones and consequences for marine ecosystems. Science 321(5891):926–929. https://doi.org/10.1126/science.1156401

Dickson AG, Millero FJ (1987) A comparison of the equilibrium constants for the dissociation of carbonic acid in seawater media. Deep-Sea Res Part A Oceanogr Res Pap 34(10):1733–1743. https://doi.org/10.1016/0198-0149(87)90021-5

Dickson AG, Sabine CL, Christian JR (2007) Guide to best practices for ocean CO_2 measurements. PICES Spec Publ 3(8):1–191. https://doi.org/10.1159/000331784

Dixon GK, Syrett PJ (1988) The growth of dinoflagellates in laboratory cultures. New Phytol 109(3):297–302. https://doi.org/10.1111/j.1469-8137.1988.tb04198.x

Doney SC, Fabry VJ, Feely RA, Kleypas JA (2009) Ocean acidification: the other CO_2 problem. Ann Rev Mar Sci 1(1):169–192. https://doi.org/10.1146/annurev.marine.010908.163834

Eberlein T, Van de Waal DB, Rost B (2014) Differential effects of ocean acidification on carbon acquisition in two bloom-forming dinoflagellate species. Physiol Plant 151(4):468–479. https://doi.org/10.1111/ppl.12137

Echigoya R, Rhodes L, Oshima Y, Satake M (2005) The structures of five new antifungal and hemolytic amphidinol analogs from *Amphidinium carterae* collected in New Zealand. Harmful Algae 4(2):383–389. https://doi.org/10.1016/j.hal.2004.07.004

Finazzi G, Furia A, Barbagallo RP, Forti G (1999) State transitions, cyclic and linear electron transport and photophosphorylation in *Chlamydomonas reinhardtii*. Biochim Biophys Acta 1413:117–129. https://doi.org/10.1016/S0005-2728(99)00089-4

Finazzi G, Moreau H, Bowler C (2010) Genomic insights into photosynthesis in eukaryotic phytoplankton. Trends Plant Sci 15(10):565–572. https://doi.org/10.1016/j.tplants.2010.07.004

Foyer CH, Noctor G (2000) Tansley review No. 112. Oxygen processing in photosynthesis: regulation and signaling. New Phytol 146(3):359–388. https://doi.org/10.1046/j.1469-8137.2000.00667.x

Fu FX, Zhang Y, Warner ME, Feng Y, Sun J, Hutchins DA (2008) A comparison of future increased CO_2 and temperature effects on sympatric *Heterosigma akashiwo* and *Prorocentrum minimum*. Harmful Algae 7(1):76–90. https://doi.org/10.1016/j.hal.2007.05.006

Fu FX, Tatters AO, Hutchins DA (2012) Global change and the future of harmful algal blooms in the ocean. Mar Ecol Prog Ser 470:207–233. https://doi.org/10.3354/meps10047

Gobler CJ, Baumann H (2016) Hypoxia and acidification in ocean ecosystems: coupled dynamics and effects of marine life. Biol Lett 12(5):20150976. https://doi.org/10.1098/rsbl.2015.0976

Gobler CJ, DePasquale EL, Griffith AW, Baumann H (2014) Hypoxia and acidification have additive and synergistic negative effects on the growth, survival, and metamorphosis of early life stage bivalves. PLoS One 9(1):1–10. https://doi.org/10.1371/journal.pone.0083648

Godaux D, Bailleul B, Berne N, Cardol P (2015) Induction of photosynthetic carbon fixation in anoxia relies on hydrogenase activity and proton-gradient regulation-like-mediated cyclic electron flow in *Chlamydomonas reinhardtii*. Plant Physiol 168(2):648–658. https://doi.org/10.1104/pp.15.00105

Goldman JAL, Bender ML, Morel FMM (2017) The effects of pH and pCO_2 on photosynthesis and respiration in the diatom *Thalassiosira weissflogii*. Photosynth Res 132(1):83–93. https://doi.org/10.1007/s11120-016-0330-2

Gonzàlez-Meler MA, Ribas-Carbó M, Siedow JN, Drake BG (1996) Direct inhibition of plant mitochondrial respiration by elevated CO_2. Plant Physiol 112(3):1349–1355. https://doi.org/10.1104/pp.112.3.1349

Gruber N (2011) Warming up, turning sour, losing breath: ocean biogeochemistry under global change. Phil Trans R Soc 369:1980–1996. https://doi.org/10.1098/rsta.2011.0003

Gruber RK, Lowe RJ, Falter JL (2017) Metabolism of a tide-dominated reef platform subject to extreme diel temperature and oxygen variations. Limnol Oceanogr 62(4):1701–1717. https://doi.org/10.1002/lno.10527

Guillard RRL, Hargraves PE (1993) *Stichochrysis immobilis* is a diatom, not a chrysophyte. Phycologia 32(3):234–236. https://doi.org/10.2216/i0031-8884-32-3-234.1

Guinotte JM, Fabry VJ (2008) Ocean acidification and its potential effects on marine ecosystems. Ann N Y Acad Sci 1134(1):320–342. https://doi.org/10.1196/annals.1439.013

Hackenberg C, Engelhardt A, Matthijs HCP, Wittink F et al (2009) Photorespiratory 2-phosphoglycolate metabolism and photoreduction of O_2 cooperate in high-light acclimation of *Synechocystis* sp. strain PCC 6803. Planta 230(4):625–637. https://doi.org/10.1007/s00425-009-0972-9

Hargraves PE, Maranda L (2002) Potentially toxic or harmful microalgae from the northeast coast. Northeast Nat 9(1):81–120. https://doi.org/10.2307/3858576

Hattenrath-Lehmann TK, Smith JL, Wallace RB, Merlo LR et al (2015) The effects of elevated CO_2 on the growth and toxicity of field populations and cultures of the saxitoxin-producing dinoflagellate *Alexandrium fundyense*. Limnol Oceanogr 60(1):198–214. https://doi.org/10.1002/lno.10012

Hennon GMM, Hernández Limón MD, Haley ST, Juhl AR, Dyhrman ST (2017) Diverse CO_2-induced responses in physiology and gene expression among eukaryotic phytoplankton. Front Microbiol 8:1–14. https://doi.org/10.3389/fmicb.2017.02547

Huang S-J, Kuo C-M, Lin Y-C, Chen Y-M, Lu C-K (2009) Carteraeol E, a potent polyhydroxyl ichthyotoxin from the dinoflagellate *Amphidinium carterae*. Tetrahedron Lett 50(21):2512–2515. https://doi.org/10.1016/j.tetlet.2009.03.065

Hulburt EM (1957) The taxonomy of unarmored Dinophyceae of shallow embayments on Cape Cod, Massachusetts. Biol Bull 112(2):196–219. https://doi.org/10.2307/1539198

IPCC (2013) Long-term climate change: projections, commitments and irreversibility. In: Stocker TF, Qin D, Plattner GK, Tignor M et al (eds) Climate change 2013: the physical science basis. Contribution of Working Group I to the Fifth Assessment Report of the Intergovernmental Panel on Climate Change. Cambridge University Press, Cambridge, pp 1029–1136

Jampeetong A, Brix H (2009) Oxygen stress in *Salvinia natans*: interactive effects of oxygen availability and nitrogen source. Envir Exp Bot 66(2):153–159. https://doi.org/10.1016/j.envexpbot.2009.01.006

Jenks A, Gibbs SP (2000) Immunolocalization and distribution of Form II RuBisCO in the pyrenoid and chloroplast stroma of *Amphidinium carterae* and Form I RuBisCO in the symbiont-derived plastics of *Peridinium foliaceum* (Dinophyceae). J Phycol 36(1):127–138. https://doi.org/10.1046/j.1529-8817.2000.99114.x

Jones RJ, Hoegh-Guldberg O (2001) Diurnal changes in the photochemical efficiency of the symbiotic dinoflagellates (Dinophyceae) of corals: photoprotection, photoinactivation and the relationship to coral bleaching. Plant Cell Environ 24:89–99. https://doi.org/10.1046/j.1365-3040.2001.00648.x

Juhl AR, Latz MI (2002) Mechanisms of fluid shear-induced inhibition of population growth in a red-tide dinoflagellate. J Phycol 38(4):683–694. https://doi.org/10.1046/j.1529-8817.2002.00165.x

Keeling RF, Körtzinger A, Gruber N (2010) Ocean deoxygenation in a warming world. Annu Rev Mar Sci 2(1):199–229. https://doi.org/10.1146/annurev.marine.010908.163855

Kitaya Y, Xiao L, Masuda A, Ozawa T, Tsuda M, Omasa K (2008) Effects of temperature, photosynthetic photon flux density, photoperiod and O_2 and CO_2 concentrations on growth rates of the symbiotic dinoflagellate, Amphidinium sp. J Appl Phycol 20(5):737–742. https://doi.org/10.1007/s10811-008-9331-7

Kroeker KJ, Kordas RL, Crim R, Hendriks IE et al (2013) Impacts of ocean acidification on marine organisms: quantifying sensitivities and interaction with warming. Glob Change Biol 19(6):1884–1896. https://doi.org/10.1111/gcb.12179

Laws EA, Bidigare RR, Popp BN (1997) Effect of growth rate and CO_2 concentration on carbon isotopic fractionation by the marine diatom *Phaeodactylum tricornutum*. Limnol Oceanogr 42(7):1552–1560. https://doi.org/10.4319/lo.1997.42.7.1552

Leggat W, Badger MR, Yellowlees D (1999) Evidence for an inorganic carbon-concentrating mechanism in the symbiotic dinoflagellate *Symbiodinium* sp. Plant Physiol 121:1247–1255. https://doi.org/10.1104/pp.121.4.1247

Li G, Campbell DA (2017) Interactive effects of nitrogen and light on growth rates and RuBisCO content of small and large centric diatoms. Photosynth Res 131(1):93–103. https://doi.org/10.1007/s11120-016-0301-7

Liu N, Beardall J, Gao K (2017) Elevated CO_2 and associated seawater chemistry do not benefit a model diatom grown with increased availability of light. Aquat Microb Ecol 79(2):137–147. https://doi.org/10.3354/ame01820

Loganathan N, Tsai Y-CC, Mueller-Cajar O (2016) Characterization of the heterooligomeric red-type RuBisCO activase from red algae. Proc Natl Acad Sci 113(49):14019–14024. https://doi.org/10.1073/pnas.1610758113

Losh JL, Young JN, Morel FMM (2013) RuBisCO is a small fraction of total protein in marine phytoplankton. New Phytol 198(1):52–58. https://doi.org/10.1111/nph.12143

Mehrbach C, Culberson CH, Hawley JE, Pytkowicx RM (1973) Measurement of the apparent dissociation constants of carbonic acid in seawater at atmospheric pressure. Limnol Oceanogr 18(6):897–907. https://doi.org/10.4319/lo.1973.18.6.0897

Melzner F, Thomsen J, Koeve W, Oschlies A et al (2013) Future ocean acidification will be amplified by hypoxia in coastal habitats. Mar Biol 160(8):1875–1888. https://doi.org/10.1007/s00227-012-1954-1

Murray SA, Garby T, Hoppenrath M, Neilan BA (2012) Genetic diversity, morphological uniformity and polyketide production in dinoflagellates (*Amphidinium*, Dinoflagellata). PLoS One 7(6):1–14. https://doi.org/10.1371/journal.pone.0038253

Parry MAJ, Keys AJ, Madgwick PJ, Carmo-Silva AE, Andralojc PJ (2008) RuBisCO regulation: a role for inhibitors. J Exp Bot 59(7):1569–1580. https://doi.org/10.1093/jxb/ern084

Peckol P, Rivers JS (1995) Physiological responses of the opportunistic macroalgae *Cladophora vagabunda* (L.) van den Hoek and *Gracilaria tikvahiae* (McLachlan) to environmental disturbances associated with eutrophication. J Exp Mar Biol Ecol 190(1):1–16. https://doi.org/10.1016/0022-0981(95)00026-n

Peltier G, Thibault P (1983) Ammonia exchange and photorespiration in *Chlamydomonas*. Plant Physiol 71(4):888–892. https://doi.org/10.1104/pp.71.4.888

Peñuelas J, Llusià J (2002) Linking photorespiration, monoterpenes and thermotolerance in *Quercus*. New Phytol 155(2):227–237. https://doi.org/10.1046/j.1469-8137.2002.00457.x

Peterhansel C, Horst I, Niessen M, Blume C et al (2010) Photorespirations. Arabidopsis Book 8(e0130):1–24. https://doi.org/10.1199/tab.0130

Pierangelini M, Raven JA, Giordano M (2017) The relative availability of inorganic carbon and inorganic nitrogen influences the response of the dinoflagellate *Protoceratium reticulatum* to elevated CO_2. J Phycol 53:298–307. https://doi.org/10.1111/jpy.12463

Pope DH (1975) Effects of light intensity, oxygen concentration, and carbon dioxide concentration on photosynthesis in algae. Microb Ecol 2(1):1–16. https://doi.org/10.1007/BF02010377

Possmayer M, Berardi G, Beall BFN, Trick CG, Hüner NPA, Maxwell DP (2011) Plasticity of the psychrophilic green alga *Chlamydomonas raudensis* (UWO 241) (Chlorophyta) to supraoptimal temperature stress. J Phycol 47(5):1098–1109. https://doi.org/10.1111/j.1529-8817.2011.01047.x

Rabalais NN, Díaz RJ, Levin LA, Turner RE, Gilbert D, Zhang J (2010) Dynamics and distribution of natural and human-caused hypoxia. Biogeosciences 7(2):585–619. https://doi.org/10.5194/bg-7-585-2010

Ratti S, Giordano M, Morse D (2007) CO_2-concentrating mechanisms of the potentially toxic dinoflagellate *Protoceratium reticulatum* (Dinophyceae, Gonyaulacales). J Phycol 43:693–701. https://doi.org/10.1111/j.1529-8817.2007.00368.x

Raven JA (2013) RuBisCO: still the most abundant protein of Earth? New Phytol 198:1–3. https://doi.org/10.1111/nph.12197

Raven JA, Cockell CS, De La Rocha CL (2008) The evolution of inorganic carbon concentrating mechanisms in photosynthesis. Phil Trans R Soc B 363:2641–2650. https://doi.org/10.1098/rstb.2008.0020

Riebesell U, Fabry VJ, Hansson L, Gattuso J-P (2011) Guide to best practices for ocean acidification research and data reporting. European Commission, Luxembourg, pp 1–258. https://doi.org/10.2777/66906

Robbins LL, Hansen ME, Kleypas JA, Meylan SC (2010) CO_2calc: a user-friendly seawater carbon calculator for Windows, Max OS X, and iOS (iPhone). US Geol Surv, pp 1–17

Roberty S, Bailleul B, Berne N, Franck F, Cardol P (2014) PSI Mehler reaction is the main alternative photosynthetic electron pathway in *Symbiodinium* sp., symbiotic dinoflagellates of cnidarians. New Phytol 204:81–91. https://doi.org/10.1111/nph.12903

Schreiber U, Vidaver W (1974) Chlorophyll fluorescence induction in anaerobic *Scenedesmus obliquus*. Biochim Biophys Acta 368(1):97–112. https://doi.org/10.1016/0005-2728(74)90100-5

Schreiber U, Neubauer C, Schliwa U (1993) PAM fluorometer based on medium-frequency pulsed Xe-flash measuring light: a highly sensitive new tool in basic and applied photosynthesis research. Photosynth Res 36(1):65–72. https://doi.org/10.1007/BF00018076

Sobrino C, Ward ML, Neale PJ (2008) Acclimation to elevated carbon dioxide and ultraviolet radiation in the diatom *Thalassiosira pseudonana*: effects on growth, photosynthesis, and spectral sensitivity of photoinhibition. Limnol Oceanogr 53(2):494–505. https://doi.org/10.4319/lo.2008.53.2.0494

Steidinger KA, Jangen K (1996) Dinoflagellates. In: Tomas CR (ed) Identifying marine phytoplankton. Academic Press, New York, pp 387–589

Strickland JDH, Parsons TR (1972) A practical handbook of seawater analysis, 2nd edn. Fisheries Research Board of Canada Bulletin, Ottawa, pp 1–310. https://doi.org/10.1002/iroh.19700550118

Sunda WG, Cai W-J (2012) Eutrophication induced CO_2-acidification of subsurface coastal waters: interactive effects of temperature, salinity, and atmospheric pCO_2. Envir Sci Tech 46(19):10651–10659. https://doi.org/10.1021/es300626f

Tabita FR, Hanson TE, Li H, Satagopan S, Singh J, Chan S (2007) Function, structure, and evolution of the RuBisCO-like proteins and their RuBisCO homologs. Microbiol Mol Biol R 71(4):576–599. https://doi.org/10.1128/MMBR.00015-07

Takahashi S, Bauwe H, Badger M (2007) Impairment of the photorespiratory pathway accelerates photoinhibition of photosystem II by suppression of repair but not acceleration of damage processes in Arabidopsis. Plant Physiol 144(1):487–494. https://doi.org/10.1104/pp.107.097253

Takeba G, Kozaki A (1998) Photorespiration is an essential mechanism for the protection of C_3 plants from photooxidation. In: Satoh K, Murata N (eds) stress responses of photosynthetic organisms. Elsevier, Amsterdam, pp 15–36

Tcherkez G, Bligny R, Gout E, Mahé A, Hodges M, Cornic G (2008) Respiratory metabolism of illuminated leaves depends on CO_2 and O_2 conditions. Proc Natl Acad Sci 105(2):797–802. https://doi.org/10.1073/pnas.0708947105

Tortell PD (2000) Evolutionary and ecological perspectives on carbon acquisition in phytoplankton. Limnol Oceanogr 45(3):744–750. https://doi.org/10.4319/lo.2000.45.3.0744

Ulstrup KE, Hill R, Ralph PJ (2005) Photosynthetic impact of hypoxia on *in hospite* zooxanthellae in the scleractinian coral *Pocillopora damicornis*. Mar Ecol Prog Ser 286:125–132. https://doi.org/10.3354/meps286125

Vaquer-Sunyer R, Duarte CM (2008) Thresholds of hypoxia for marine biodiversity. Proc Natl Acad Sci 105(40):15452–15457. https://doi.org/10.1073/pnas.0803833105

Wallace RB, Baumann H, Grear JS, Aller RC, Gobler CJ (2014) Coastal ocean acidification: the other eutrophication problem. Estuar Coast Shelf Sci 148:1–13. https://doi.org/10.1016/j.ecss.2014.05.027

Whitney SM, Andrews TJ (1998) The CO_2/O_2 specificity of single-subunit ribulose-bisphosphate carboxylase from the dinoflagellate, *Amphidinium carterae*. Aust J Plant Physiol 25:131–138. https://doi.org/10.1071/PP97167

Wu Y, Gao K, Riebesell U (2010) CO_2-induced seawater acidification affects physiological performance of the marine diatom *Phaeodactylum tricornutum*. Biogeosciences 7(9):2915–2923. https://doi.org/10.5194/bg-7-2915-2010

Wu RSS, Wo KT, Chiu JMY (2012) Effects of hypoxia on growth of the diatom *Skeletonema costatum*. J Exp Mar Biol Ecol 420–421:65–68. https://doi.org/10.1016/j.jembe.2012.04.003

Young JN, Goldman JAL, Kranz SA, Tortell PD, Morel FMM (2015a) Slow carboxylation of RuBisCO constrains the rate of carbon fixation during Antarctic phytoplankton blooms. New Phytol 205(1):172–181. https://doi.org/10.1111/nph.13021

Young JN, Kranz SA, Goldman JAL, Tortell PD, Morel FMM (2015b) Antarctic phytoplankton down-regulate their carbon-concentrating mechanisms under high CO_2 with no change in growth rates. Mar Ecol Prog Ser 532:13–28. https://doi.org/10.3354/meps11336

Young JN, Heureux AMC, Sharwood RE, Rickaby REM, Morel FMM, Whitney SM (2016) Large variation in the RuBisCO kinetics of diatoms reveals diversity among their carbon-concentrating mechanisms. J Exp Bot 67(11):3445–3456. https://doi.org/10.1093/jxb/erw163